PB-234 975

URBAN AIR SHED PHOTOCHEMICAL SIMULATION MODEL STUDY

VOLUME I. DEVELOPMENT AND EVALUATION. APPENDIX B. GENERALIZED MECHANISM FOR DESCRIBING ATMOSPHERIC PHOTOCHEMICAL REACTIONS

SYSTEMS APPLICATIONS, INCORPORATED

PREPARED FOR
ENVIRONMENTAL PROTECTION AGENCY

JULY 1973

DISTRIBUTED BY:
NTIS
National Technical Information Service
U. S. DEPARTMENT OF COMMERCE

BIBLIOGRAPHIC DATA SHEET	1. Report No. EPA-R4-73-030c	2.	PB 234 975

4. Title and Subtitle
Urban Air Shed Photochemical Simulation Model Study Volume I - Development and Evaluation Appendix B - Generalized Mechanism for Describing Atmospheric Photochemical Reactions

5. Report Date July 1973

6.

7. Author(s)
T. A. Hecht

8. Performing Organization Rept. No.

9. Performing Organization Name and Address
Systems Applications, Inc.
9418 Wilshire Boulevard
Beverly Hills, California 90212

10. Project/Task/Work Unit No.

11. Contract/Grant No.
68-02-0339

12. Sponsoring Organization Name and Address
U.S. ENVIRONMENTAL PROTECTION AGENCY
Office of Research and Development
Washington, D. C. 20460

13. Type of Report & Period Covered

14.

15. Supplementary Notes

16. Abstracts
The aims were: to modify the treatment of nitrous acid in the mechanism, to include additional categories of lumped hydrocarbons and their reactions, to improve means for estimating the generalized stoichiometric coefficients, and most importantly, to assess more fully the mechanism's validity. Validity of the mechanism, as modified, was carried out for a variety of reactive systems, including single hydrocarbons, binary mixtures, and auto exhaust. The mechanism provides an adequate, perhaps good, description of smog chamber kinetics. In particular, the model appears capable of predicting the concentration/time behavior of a variety of reactant systems over a wide range of initial conditions. The few auto exhaust simulations performed indicate that the mechanism displays promise for describing the complex mixtures that exist in the atmosphere. The guidelines established for estimating rate constants and stoichiometric coefficients also have proven to be quite adequate.

17. Key Words and Document Analysis. 17a. Descriptors

Air pollution	Nitrogen dioxide	Toluene
Urban areas	Ozone	Motor vehicles
Photochemical reactions	Particles	Exhaust emissions
Simulation	Light (visible radiation)	Propylene
Mathematical models	Water	
Reaction kinetics	Vapors	
Hydrocarbons	Nitric acid	
Atmospheric diffusion	Nitrous acid	
Carbon monoxide	Catalysis	
Nitrogen oxide (NO)	Tests	

RECEIVED
JAN 25 1974

17b. Identifiers/Open-Ended Terms

Reproduced by
NATIONAL TECHNICAL
INFORMATION SERVICE
U S Department of Commerce
Springfield VA 22151

17c. COSATI Field/Group 13B

18. Availability Statement	19. Security Class (This Report)	21. No. of Pages
Unlimited	UNCLASSIFIED	88
	20. Security Class (This Page) UNCLASSIFIED	22. Price $4.00-1.45

EPA-R4-73-030c

URBAN AIR SHED PHOTOCHEMICAL SIMULATION MODEL STUDY

VOLUME I - DEVELOPMENT AND EVALUATION

Appendix B - Generalized Mechanism for Describing Atmospheric Photochemical Reactions

by

T.A. Hecht

Systems Applications, Inc.
9418 Wilshire Boulevard
Beverly Hills, California 90212

Contract No. 68-02-0339
Program Element No. 1A1009

EPA Project Officer: Herbert Viebrock

Meteorology Laboratory
National Environmental Research Center
Research Triangle Park, North Carolina 27711

Prepared for

OFFICE OF RESEARCH AND DEVELOPMENT
U.S. ENVIRONMENTAL PROTECTION AGENCY
WASHINGTON, D.C. 20460

July 1973

ia

This report has been reviewed by the Environmental Protection Agency and approved for publication. Approval does not signify that the contents necessarily reflect the views and policies of the Agency, nor does mention of trade names or commercial products constitute endorsement or recommendation for use.

ACKNOWLEDGMENTS

We wish to thank Dr. Marcia Dodge of E.P.A. for many helpful discussions concerning modeling of the auto exhaust data, particularly with regard to establishing the hydrocarbon concentrations and definitizing the roles of particles and carbon monoxide. We also acknowledge Dr. S. L. Kopczynski of E.P.A. for his aid in clarifying a number of experimental and analytical details related to the data base.

CONTENTS

		Page
I.	PURPOSE OF WORK	B-1
II.	THE KINETIC MECHANISM	B-3
	A. The Treatment of HNO_2	B-3
	B. Hydrocarbon Mixtures	B-9
	C. Reactions Involving Particles	B-10
	D. Dilution Effects	B-10
	E. The Constancy of Stoichiometric Coefficients	B-11
	F. The Reaction Rate Constants	B-11
III.	THE DATA BASE AND SOURCES OF EXPERIMENTAL UNCERTAINTY	B-12
	A. The Data Base	B-12
	B. Light Intensity	B-14
	C. Water Vapor in Chamber	B-15
	D. Walls Effects	B-15
	1. NO and NO_2	B-16
	2. N_2O_5	B-16
	3. HNO_3	B-18
	4. Other Chemical and Catalytic Effects of the Walls	B-18
	5. Conclusions	B-19
	E. Estimates of Experimental Error	B-19
	1. The Accuracy of the Analytical Instruments	B-20
	2. The Repeatability of Experimental Runs	B-21

CONTENTS (Continued)

		Page
IV.	VALIDATION OF THE MECHANISM	B-24
	A. Estimation of Parameters	B-24
	1. The Rate Constants	B-24
	2. Generalized Stoichiometric Coefficients	B-27
	3. Sensitivity of the Model to Variations in the Magnitudes of Parameters	B-29
	B. The Validation Results	B-32
	1. Toluene-NO_x Validation	B-32
	2. Toluene-n-Butane-NO_x Validations	B-35
	3. Propylene-Ethane-NO_x Validations	B-47
	4. Auto Exhaust Validations	B-55
V.	CONCLUDING COMMENTS	B-75
	REFERENCES	B-79

√

LIST OF TABLES

		Page
1.	The Generalized Photochemical Kinetic Mechanism	B-4
2.	Mathematical Representation of the Kinetic Mechanism	B-6
3.	Initial Conditions Associated with Experimental Chamber Data	B-13
4.	Precision Bounds (90% Confidence Levels) for Toluene-NO_x and Toluene-n-Butane-NO_x Data	B-22
5.	Sensitivity of the Model to Light Intensity, Water Concentration, and Initial NO_2 Concentration	B-31
6.	List of Figures	B-33
7.	Key to Figures	B-34
8.	Validation Parameters for Toluene-NO_x Experiments	B-36
9.	Validation Parameters for Toluene-n-Butane-NO_x Experiments	B-48
10.	Validation Parameters for Propylene-Ethane-NO_x Experiments	B-56
11.	Values of Base Parameters Used to Calculate Rate Constants and Stoichiometric Coefficients for Complex Hydrocarbon Mixtures	B-68
12.	Validation Parameters for Auto Exhaust Experiments (Unequipped Chevelle)	B-71
13.	Validation Parameters for Auto Exhaust Experiments (Equipped Chevelle)	B-72

I. PURPOSE OF WORK

The main purpose of the current contract effort is the development and validation of a simulation model for estimating ground level concentrations of photochemical pollutants. A major component of the model is a generalized kinetic mechanism capable of describing atmospheric chemical reactions. Before a kinetic mechanism can be included in an airshed simulation, however, its validity must be established by comparing its predictions with concentration/time profiles observed under controlled laboratory conditions; i.e., smog chamber experiments.*

During the first phase of model development, under Contract CPA 70-148, we undertook to identify an existing kinetic mechanism, or, if necessary, to develop a new mechanism, capable of meeting the following requirements for inclusion in an atmospheric simulation: relative simplicity (in the interest of minimizing requisite calculations), sufficient generality to include all major gaseous contaminant species (aerosols were not considered in the study), and acceptable accuracy in the prediction of smog chamber data over a range of values of HC/NO_x ratios and for a variety of hydrocarbons. Initially, we carried out an assessment of existing mechanisms, and we concluded that a "better" model was needed. At about that time, a program to develop such a model was being initiated under the aegis of Prof. John H. Seinfeld at the California Institute of Technology. It became clear at an early stage of that work that the mechanism being formulated at Caltech represented a significant advance in the field. We adopted the new mechanism and carried out a series of validation runs which are detailed in Seinfeld, et al. (1971). The results demonstrated that this model is capable of predicting with acceptable accuracy the concentration/time behavior of smog chamber experiments for propylene, isobutylene, n-butane, and a mixture of propylene and n-butane at initial NO_x to hydrocarbon ratios of 1/3 to 1. The mechanism was also shown to simulate accurately the effect on photooxidation rates of variations in CO concentration, as well as the inhibitory effect of high initial concentrations of nitric oxide on the maximum concentration of ozone obtained.

---

* The attainment of acceptable validation of the model using smog chamber data does not necessarily imply that the mechanism is capable of simulating actual atmospheric processes. Certain physical and chemical attributes of the atmospheric mixture are not simulated in laboratory studies. In particular, aerosols and particulates found in the atmosphere undoubtedly influence chemical processes. As their density, number and size distribution and chemical composition remain highly uncertain, their effect on rate processes remains unknown.

Despite the generally favorable character of the results of this study, further work was needed. We wished to modify the treatment of nitrous acid in the mechanism, to include additional categories of lumped hydrocarbons and their reactions, and to improve means for estimating the generalized stoichiometric coefficients. Most importantly, however, we wished to assess more fully the mechanism's validity. It was the purpose of this effort to carry out validation of the mechanism, as modified, for a variety of reactive systems, including single hydrocarbons, binary mixtures, and auto exhaust. If validation were adjudged "successful", the mechanism could then be considered for incorporation into the urban airshed model. We herein report the results of this study.

II. THE KINETIC MECHANISM

The kinetic mechanism, given in Table 1, has been discussed in detail in Seinfeld, et al. (1971). The mechanism consists of fifteen reactions involving ten chemical species. The mathematical representation includes four differential equations to permit prediction of the change in concentration with time of NO , NO_2 , ozone, and hydrocarbons. Five of the species, all radicals, react rapidly to establish equilibrium concentrations and can thus be represented by algebraic equations. These species are O , OH , HO_2 , RO_2 and NO_3 . The tenth species HNO_2 has been treated as if the steady state approximation were valid for its reactions, although this is known not to be the case. We will discuss the basis for this assumption later in this section. Thus, four differential equations and six algebraic equations, given in Table 2, embody the complete mathematical statement of the mechanism.

As noted, we have discussed the mechanism fully in our previous report. We thus limit the discussion of this section to a description of modifications of the original formulation.

A. The Treatment of HNO_2

The original formulation of the kinetic mechanism [Hecht and Seinfeld (1972)] included a differential equation to describe the variation in HNO_2 concentration with time. This species, however, is not of major importance in the urban airshed model, is not measured in the atmosphere, and is not, in fact, listed among those pollutants for which air quality standards have been written. The urban airshed model, as formulated, requires the integration of the coupled, time-dependent, partial differential equations of conservation of mass for NO , NO_2 , ozone, and hydrocarbon. Inclusion of a fifth equation for HNO_2 would increase computing time by 20 to 25% and would also increase computer storage requirements.

While we were well aware of the fact that HNO_2 concentration varies with time, we thought it would be worthwhile to explore the possibility of introducing the artifact of a steady-state assumption in describing the concentration of this species, achieving the necessary scaling by suitably modifying the reaction rate constant. Two questions immediately arise: (1) Is such an assumption justifiable?, and (2) If it is justifiable, is it warranted?

The justifiability of the assumption can be argued on two grounds. First, the term dc_{HNO_2}/dt is quite sensitive to changes in the magnitude of k_6 and water concentration in the reaction

$$NO + NO_2 \xrightarrow[H_2O]{6} 2HNO_2$$

TABLE 1. The Generalized Photochemical Kinetic Mechanism

The Basic 15-Step Mechanism

$$NO_2 + h\nu \xrightarrow{1} NO + O$$

$$O + O_2 + M \xrightarrow{2} O_3 + M$$

$$O_3 + NO \xrightarrow{3} NO_2 + O_2$$

$$O_3 + NO_2 \xrightarrow{4} NO_3 + O_2$$

$$NO_3 + NO_2 \xrightarrow[H_2O]{5} 2\ HNO_3$$

$$NO + NO_2 \xrightarrow[H_2O]{6} 2\ HNO_2$$

$$HNO_2 + h\nu \xrightarrow{7} OH + NO$$

$$CO + OH \xrightarrow[O_2]{8} CO_2 + HO_2$$

$$HO_2 + NO \xrightarrow{9} OH + NO_2$$

$$HO_2 + NO_2 \xrightarrow{10} HNO_2 + O_2$$

$$HC + O \xrightarrow{11} \alpha RO_2$$

$$HC + OH \xrightarrow{12} \beta RO_2$$

$$HC + O_3 \xrightarrow{13} \gamma RO_2$$

$$RO_2 + NO \xrightarrow{14} NO_2 + \varepsilon OH$$

$$RO_2 + NO_2 \xrightarrow{15} PAN$$

TABLE 1. (Continued)

Additional Reactions Considered in This Study

$$HC_2 + O \xrightarrow{16} \alpha_2 RO_2$$

$$HC_2 + OH \xrightarrow{17} \beta_2 RO_2$$

$$HC_2 + O_3 \xrightarrow{18} \gamma_2 RO_2$$

$$NO_2 + \text{PARTICLE} \xrightarrow{19} \text{NITRATE}$$

TABLE 2. The Mathematical Representation of the Kinetic Mechanism

Rates of the Reactions:

$$r_1 = k_1 \cdot NO_2$$
$$r_2 = k_2 \cdot O \quad \dagger$$
$$r_3 = k_3 \cdot O_3 \cdot NO$$
$$r_4 = k_4 \cdot O_3 \cdot NO_2$$
$$r_5 = k_5 \cdot NO_3 \cdot NO_2 \quad \dagger\dagger$$
$$r_6 = k_6 \cdot NO \cdot NO_2 \quad \dagger\dagger$$
$$r_7 = k_7 \cdot HNO_2$$
$$r_8 = k_8 \cdot OH \quad \dagger$$
$$r_9 = k_9 \cdot HO_2 \cdot NO$$
$$r_{10} = k_{10} \cdot HO_2 \cdot NO_2$$
$$r_{11} = k_{11} \cdot HC \cdot O$$
$$r_{12} = k_{12} \cdot HC \cdot OH$$
$$r_{13} = k_{13} \cdot HC \cdot O_3$$
$$r_{14} = k_{14} \cdot RO_2 \cdot NO$$
$$r_{15} = k_{15} \cdot RO_2 \cdot NO_2$$
$$r_{16} = k_{16} \cdot HC_2 \cdot O$$
$$r_{17} = k_{17} \cdot HC_2 \cdot OH$$
$$r_{18} = k_{18} \cdot HC_2 \cdot O_3$$
$$r_{19} = k_{19} \cdot NO_2$$

Differential Equations:

$$\frac{dNO_2}{dt} = -r_1 + r_3 - r_4 - r_5 - r_6 + r_9 - r_{10} + r_{14} - r_{15} - r_{19}$$

$$\frac{dNO}{dt} = r_1 - r_3 - r_6 + r_7 - r_9 - r_{14}$$

$$\frac{dO_3}{dt} = r_2 - r_3 - r_4 - r_{13} - r_{18}$$

$$\frac{dHC}{dt} = - r_{11} - r_{12} - r_{13}$$

$$\frac{dHC_2}{dt} = - r_{16} - r_{17} - r_{18}$$

---

† pseudo first order reaction
†† pseudo second order reaction

TABLE 2. (Continued)

Algebraic Steady State Equations:

$$(NO_3) = \frac{k_4}{k_5}(O_3)$$

$$(O) = \frac{k_1(NO_2)}{k_2 + k_{11}(HC) + k_{16}(HC_2)}$$

$$(RO_2\cdot) = \frac{DF - EB}{\varepsilon E k_{14}(NO) + CF}$$

where $B = 2k_6(NO)(NO_2)$

$$C = -\left[k_{14}(NO) + k_{15}(NO_2)\right]$$

$$D = -\left[\alpha k_{11}(HC)(O) + \gamma k_{13}(HC)(O_3) + \alpha_2 k_{16}(HC_2)(O) + \gamma_2 k_{18}(HC_2)(O_3)\right]$$

$$E = \beta k_{12}(HC) + \beta_2 k_{17}(HC_2)$$

$$F = k_{12}(HC) + k_{17}(HC_2)$$

$$(\cdot OH) = \frac{2k_6(NO)(NO_2) + \varepsilon k_{14}(RO_2\cdot)(NO)}{k_{12}(HC) + k_{17}(HC_2)}$$

$$(HO_2\cdot) = \frac{k_8(OH\cdot)}{k_{10}(NO_2) + k_9(NO)}$$

$$(HNO_2) = \frac{k_{10}(HO_2)(NO_2) + 2k_6(NO)(NO_2)}{k_7}$$

and to k_7 in the reaction

$$HNO_2 + h\nu \xrightarrow{7} OH + NO \quad .$$

k_6 has not yet been accurately determined, water concentration was not controlled with care during the experimental program, and k_7, which depends on light intensity, is not well known. Thus, dc_{HNO_2}/dt can be determined only with considerable uncertainty. (This does not, however, imply that its magnitude is negligible.) Second, there are absolutely no measurements of HNO_2; thus, there is no way to verify predicted values of HNO_2 concentration.

In light of these considerations and due to our desire to avoid the inclusion of an additional partial differential equation in the airshed model, we decided to investigate the effects of invoking the steady-state assumption for HNO_2. In particular:

(a) If the assumption were made, what effect would it have on predicted concentration/time profiles for NO, NO_2 ozone, and hydrocarbon?

(b) Assuming the effect were small, what modifications, if any, in the value of k_6 would be needed? Would it be possible to establish a value, $\rho = (\tilde{k}_6/k_6)$, where $\tilde{k}_6$ is the pseudo rate constant that yields HNO_2 vs. time profiles under the steady-state assumption that closely match the profiles computed when the differential equation for HNO_2 was included in the formulation?

If the NO, NO_2, O_3, and hydrocarbon concentration/time profiles could be duplicated, or nearly duplicated, under the steady-state assumption by adopting a rate constant, $\tilde{k}_6 = \rho k_6$, which was invariant, or nearly so, for the various reaction systems of interest, we felt that the steady-state assumption was then both justifiable and warranted.

In order to investigate the appropriateness of the steady-state assumption we carried out validation runs at different HC/NO_x ratios for the reactants, n-butane and n-butane-toluene. We also undertook validation for n-butane at one HC/NO_x ratio with 100 ppm of added CO. We carried out two runs for each reactant system, one including

the differential equation for HNO_2 in the model, with k_6 = .004 $ppm^{-1}min^{-1}$, and one assuming HNO_2 to be in steady state, with $\bar{k}_6 = 1/8\ k_6$ ($\rho = 1/8$). Virtually identical profiles for NO, NO_2, O_3 and HC were obtained in the two calculations over the six hour integration for each reactant. For example, for the n-butane-toluene system, the NO_2 peak occurred at 116 minutes with HNO_2 concentration variations described by a differential equation, and at 113 minutes with HNO_2 in steady state. (This reflects the low sensitivity of the model to nitrous acid (see Section IV)). In view of these results we have elected to introduce the steady-state artifact into the formulation of the mechanism in the interest of easing the computational burden associated with the urban airshed model. We do believe, however, that the inclusion of a differential equation for HNO_2 will eventually be desirable.

B. Hydrocarbon Mixtures

In order to better account for the potentially wide range of reactivity of hydrocarbon mixtures, we have introduced a modification to the basic 15 step mechanism of Table 1. The mixture is represented by two lumped hydrocarbons, a low reactivity hydrocarbon (HC) and a high reactivity hydrocarbon (HC_2). The inclusion of HC_2 creates the need for three additional reactions

$$HC_2 + O \xrightarrow{16} \alpha_2 RO_2$$

$$HC_2 + OH \xrightarrow{17} \beta_2 RO_2$$

$$HC_2 + O_3 \xrightarrow{18} \gamma_2 RO_2$$

and a fifth differential equation

$$\frac{d(HC_2)}{dt} = -(r_{16} + r_{17} + r_{18})$$

HC_2 includes all olefins, while HC is comprised of aromatics (other than benzene), acetylenes (other than C_2H_2), and C_4^+ paraffins. C_1 to C_3 paraffins, acetylene and benzene are taken to be unreactive. The representation of reactive hydrocarbons in this way enhances the accuracy of the model, especially with respect to the NO oxidation and hydrocarbon consumption rates. The division of hydrocarbons by class and the assignment of rate constants and stoichiometric coefficients is discussed further under Auto Exhaust in Section IV.

C. Reactions Involving Particles

As we suggested earlier, aerosols and particles have a large influence on atmospheric chemical processes [Wilson, W.E., Jr., (1972)]. Unfortunately, little is known about the physics and chemistry of the pertinent phenomena. We do know, however, that cognizance must be given to these phenomena in order to account for the loss of NO_x prior to the NO_2 peak that is observed when particles are present in the smog chamber. We have thus included the reaction

$$NO_2 + \text{particle} \xrightarrow{19} \text{nitrate}$$

in the basic mechanism. We discuss this rate step in greater detail under Auto Exhaust in Section IV.

D. Dilution Effects

The loss of material due to sampling during experimentation is often considerable, up to 20 to 25% of the original charge. To account for this, we have included a loss term in each differential and algebraic equation. The term is of the form

$$-\frac{F}{v} c_i$$

where F = volumetric flow rate

v = volume of chamber

c_i = concentration of species i

Thus, each differential equation is of the form

$$\frac{dc_i}{dt} = f_i(c_1, c_2, \cdots, c_n) - \frac{F}{v} c_i$$

$$i = 1,2,\ldots,n$$

Note that while samples are drawn at approximately regular intervals, with no withdrawal between sampling periods, this formulation assumes continuous withdrawal at a uniform rate. This assumption was necessary, as exact information concerning withdrawal rates and periods is unavailable. The error introduced by this approximation is, however, negligible.

E. The Constancy of Stoichiometric Coefficients

In earlier validation studies of propylene-NO_x and isobutylene-NO_x we included a stoichiometric coefficient in the mechanism that varied with the ratio, (HC)/(NO) . We have since learned that the need for this variable coefficient was attributable to biases introduced into the observed results as a result of "chamber effects". As data were collected in different chambers, the "chamber effects" differ among the data sets. Also, initial conditions in many of the runs were poorly defined. In contrast, all data used for validation purposes in the current study were collected in the same smog chamber with better defined initial conditions.* In carrying out validations using these data, we have been able to establish fixed values for all stoichiometric coefficients, independent of the HC/NO_x ratio.

F. The Reaction Rate Constants

We have adopted literature values of rate constants for all inorganic reactions (with the exception of reaction 4), where these constants are known. Similarly, we have used literature values of rate constants for individual hydrocarbon reactions when possible. Specifically, we have done so for the reactions of toluene, n-butane, propylene, and ethylene with OH and ozone.** However, we have assumed values for the O-hydrocarbon reaction that are higher than those reported in the literature.

Literature values of rate constants for the inorganic reactions are given in Table B-4 of Seinfeld, et al. (1971), for the hydrocarbon reactions, in Table B-5. Constants not available in this reference may be found in Johnston, et al. (1970). Where values other than those reported in the literature have been adopted, the reasons for the selection of "new" values are given in Section IV.

---

* This, of course, suggests that a "chamber effect" may be incorporated into the estimated values of model parameters, and thus predictions of the validated mechanism may not compare as favorably with data collected in another chamber. Its applicability in the atmosphere would also be lessened due to such a bias. We discuss chamber effects in some detail in Section III of this report, and in still greater depth in a report being written under EPA Contract 68-02-0580.

** Toluene and n-butane are essentially unreactive in the presence of ozone.

III. THE DATA BASE AND SOURCES OF EXPERIMENTAL UNCERTAINTY

The significance of the validation results for a kinetic mechanism is to a large degree dependent upon the diversity and reliability of the experimental data base. We were fortunate in being able to obtain chamber runs for this study involving both low and high reactivity hydrocarbons, as well as simple mixtures and auto exhaust. Moreover, the ratio of HC/NO_x was varied over a wide range for each reactant system. In this section we describe the data base provided by the Division of Chemistry and Physics of EPA for validation purposes. We examine in some detail the importance of accurately specifying certain experimental variables, notably light intensity and water vapor concentration. We discuss the degree to which wall effects may influence observed chamber results. Finally, we comment on the accuracy and specificity of the analytical instrumentation used to monitor pollutant concentrations and present estimates of the precision with which concentrations were determined.

A. Data Base

The data base used in this validation study is that supplied by the Division of Chemistry and Physics of EPA. It is comprised of four hydrocarbon-NO_x systems:

- Toluene-NO_x at five different HC/NO_x ratios
- Toluene-n-butane-NO_x at three different HC/NO_x ratios
- Propylene-ethane-NO_x at four different HC/NO_x ratios
- Auto Exhaust at two different HC/NO_x ratios

All of the chamber runs were made between June 1966 and March 1967 by the staff of the Chemical and Physical Research and Development Program at the National Center for Air Pollution Control in Cincinnati, Ohio [Altshuller, A.P., et al. (1967a, 1967b, 1969, 1970)].

The experiments are best specified by a statement of initial conditions, as given in Table 3. Duplicate runs were carried out for all but two sets of initial conditions, these sets both being for the propylene-ethane-NO_x system. In general we chose to validate the model using that experimental run in each replicate pair

TABLE 3. Initial Conditions Associated with Experimental Chamber Data

EPA NO.	HC Type	$(NO_2)^*_o$	$(NO)^*_o$	$(HC)^*_o$
300	Toluene	.02	1.25	3.22
258	Toluene	.05	.35	2.88
250	Toluene	.04	1.17	1.53
272	Toluene	.04	.55	1.67
271	Toluene	.05	.32	1.20
251	n-Butane toluene	.07	1.10	4.62†
253	n-Butane toluene	.08	.53	4.91†
257	n-Butane toluene	.07	.27	4.26†
318	Propylene	.06	1.12	.51
325	Propylene	.04	.35	.45
321	Propylene	.10	1.31	.275
329	Propylene	.05	.26	.24
222	Auto Exhaust	.12	1.95	2.21#
231	Auto Exhaust	.23	2.80	.61#

* initial concentrations in ppm

† combined total of n-butane and toluene

\# combined total of all hydrocarbons in the auto exhaust

having the smoother concentration time profiles and the lesser loss of NO_x prior to the NO_2 peak. Experimental results displaying such anomalies as the concentration of NO exceeding that of NO_2 at the time of the NO_2 peak or the NO_2 peaking at a time when only 2/3 of the NO had been oxidized were rejected for validation purposes.

B. Light Intensity

Radiation intensity is one of the most important parameters in a smog chamber experiment, for it governs the photolysis rate of NO_2 (reaction 1), the reaction which initiates and sustains the smog formation process. Irradiation of the smog chamber was carried out through the use of two banks of externally mounted fluorescent lamps, 148 lamps of three different types. Under normal operation, these lamps have an expected lifetime of 1000 hours, but throughout the program they were operated at a 25% overvoltage to increase radiation intensity. Overload operation results in a more rapid deterioration of the lamps; consequently, approximately 1/7 of the lamps were replaced after every 100 hours of operation.

The average first order "rate constant" for NO_2 disappearance in nitrogen, k_d* , was determined by the experimenters to be 0.40 minutes^{-1}, but was not redetermined during the ten-month period over which the data provided to us were taken. We have assumed, in accordance with the results of Schuck, et al. (1966) , that k_1 , the overall photolysis rate of NO_2 , is equal to 2/3 k_d , or 0.266 minutes^{-1}. Finally, we have estimated that, due to inaccuracies in the determination of k_d , in the factor of 2/3 relating k_d to k_1 , and in the estimation of irradiation intensity, k_1 has an uncertainty bound of $\pm$ 0.10 minutes^{-1}.

---

* It can be shown that

$$k_d \sim \frac{2k_3}{k_2(M) + k_3} k_a\phi$$

where

$k_1 = k_a\phi$

k_a = photolytic absorption rate constant

ϕ = dissociation efficiency

and

$$O + NO_2 + M \xrightarrow{k_2} NO_3 + M$$

$$O + NO_2 \xrightarrow{k_3} NO + O_2$$

Thus, k_d is , in essence, a lumped parameter representing the combined rates of all NO_2 reactions in an oxygen-free atmosphere. Unfortunately, the use of k_d leads to difficulties in presenting the kinetics, as the combined reaction which it represents is not first order. However, since the only available data for light intensity in these chamber experiments are based on the validity of k_d as a rate constant, we use it here to estimate k_1 .

C. Water Vapor in Chamber

Another parameter which is thought to be important in smog chamber runs is the water concentration. Water enters into the smog kinetics via reactions 5 and 6, nitric and nitrous acid production. The latter is particularly important since photolysis of nitrous acid produces OH radicals which, in turn, initiate further reactions. The humidifier control of the inlet air stream to the chambers was set to generate 50% relative humidity at 75°F, but, during very cold, dry weather, relative humidities of only 30% were achieved. The humidity of the inlet air stream was checked only once or twice during the ten-month study. Because of the uncertainty in the water concentration for these runs, we have lumped the rate constant for reaction 6 and the water concentration into a pseudo-second order rate constant, k_6 .

In order to assess the effect of uncertainties in k_6 and/or water concentration on predicted concentration/time profiles, we carried out three sensitivity runs. The results of these runs showed that an assumed uncertainty of $\pm$ 25% in k_6 , in the water concentration, or in the lumped rate constant (all are equivalent) leads to a change of $\pm$ 4 minutes in the time to the NO_2 peak, which occurred at 112 minutes.* These reults are discussed more fully in Section IV.

In the future, it would be desirable to obtain more exact measurements of the water concentration. If such measurements become available, it would be meaningful to dispense with the lumped rate constant, treating k_6 and the water concentration individually.

D. Wall Effects

An effect of particular concern in smog chamber studies is the influence of surfaces on chemical dynamics, and thus on observed reaction kinetics. Of major importance in this regard is the possibility of direct loss of material to the walls. Of lesser concern is the possibility of chemical interactions occurring between pollutants on the walls and material in the gas phase. Although it is possible that some low reactivity organics such as carboxylic acids, aldehydes, and ketones can be found on the walls as a result of hydrogren bonding with adsorbed water, we focus our attention in this discussion on species which have been clearly identified on the walls of a small smog chamber [Gay and Bufalini (1971)] --nitric acid, nitrates, and nitrites. We begin then by discussing the reactions of the most important oxides of nitrogen, NO and NO_2 , and examining the possibility of the interaction of each with the walls. In the process we also give attention to various mechanisms that might account for the appearance of HNO_3 on the walls.

---

* Westberg (1972) has raised doubts concerning the accuracy of the only determination of k_6 [Johnston, et al. (1970)]. We have, therefore, treated the pseudo rate constant $k_6' = k_6(H_2O)$ as an adjustable parameter in our validation studies, and the low sensitivity of the time to the NO_2 peak with variations in k_6' is a reflection of our choice.

1. NO and NO_2

Even in so-called dry systems it is reasonable to assume that an adsorbed layer of water will be found on the walls of the smog chamber. This is certainly the case for the experiments under consideration in this study, as the chamber was intentionally humidified during all runs. Thus one possible explanation for the appearance of nitrate and nitrite on the walls would be dissolution of NO and NO_2 in the adsorbed water layer. Nitric oxide can be eliminated in this regard because of its extremely low solubility in water; NO_2, however, dissociates in water by the following reactions [Hill, (1971)]:

$$6NO_2 + 3H_2O \rightleftarrows 3HNO_3 + 3HNO_2$$

$$3HNO_2 \rightleftarrows HNO_3 + 2NO + H_2O \quad .$$

The rate of loss of NO_2 in this manner is dependent upon the amount of water adsorbed, the rate of dissolution of NO_2, and the magnitude of rate constants for the dissociation reactions. In the experiments under consideration, however, NO_2 losses via this mechanism can be neglected because, within experimental error, all of the NO_x initially present can be accounted for at the time of the NO_2 peak as NO_2, NO, and NO and NO_2 lost by sampling and dilution up to the time of the peak. We might then conclude that no significant amounts of NO or NO_2 were lost directly to the walls during the smog chamber experiments.

2. N_2O_5

After the NO_2 peak occurs, and as O_3 begins to accumulate, N_2O_5 forms by the reactions

$$NO_2 + O_3 \rightarrow NO_3 + O_2$$

$$NO_3 + NO_2 \rightleftarrows N_2O_5$$

N_2O_5 will undergo hydrolysis to form nitric acid by the reaction

$$N_2O_5 + H_2O \rightleftarrows 2HNO_3$$

If the hydrolysis takes place in the adsorbed layer of water on the wall, HNO_3 will form directly on the walls. However, both the water concentrations in smog chambers (63% relative humidity (RH) at 25°C is equivalent to 20,000 ppm H_2O) and the rate constants for the primary reactions in nitric acid formation in the gas phase* are large enough that the loss of NO_x after the NO_2 peak may be fully ascribed to the formation of nitric acid in the gas phase.

It remains unclear, however, as to whether N_2O_5 hydrolyzes in the gas phase or on the walls. As we have noted, the water concentration during these chamber runs was quite high. As the stationary state concentration of nitric acid** would also have been high, actual HNO_3 concentrations in these experiments were always far from saturation. Thus there would have been a strong tendency for N_2O_5, whether it were found in the gas phase or on the wall, to hydrolyze rather than to decompose, forming NO_2 by the reactions

$$N_2O_5 \rightleftarrows NO_2 + NO_3$$

$$NO_3 + NO \rightarrow 2NO_2$$

However, even if these reactions were favored due to the formation of N_2O_5, the rate of formation of NO_2 would still be low since NO is depleted at this stage of the smog reactions. Thus, in light of the various considerations presented, we conclude that reactions involving N_2O_5 at the walls would have little if any effect on the course of the overall smog reactions.

---

* See Johnston, H.S., et al. (1970) for estimates of these rate constants

** Leighton (1961), p. 193, calculates that the stationary state concentration of HNO_3 is 3,000 ppm for initial conditions of 0.10 NO_2, 0.10 O_3, 0.01 NO, and 63% RH at 25°C.

3. HNO_3

Nitric acid is very soluble in water because of strong hydrogen bonding. Thus, it is highly likely that a nitric acid molecule in the gas phase that is involved in a collision with the wall would dissolve. The rate of loss of HNO_3 from the gas phase, then, is probably transport-limited and will depend to some degree on the rate of stirring in the chamber. Unfortunately, detection of HNO_3 in the gas phase has until now proven to be a difficult task, perhaps because the acid is lost to the walls of the sampling tubes.

4. Other Chemical and Catalytic Effects of the Walls

It would be highly beneficial to gain some insight into the degree to which interactions occur between pollutants on the walls and material in the gas phase. Unfortunately, our knowledge concerning such phenomena is limited, and we can only speculate. We thus offer the following comments:

- It is expected that, for a chamber having a small surface to volume ratio, such as the one employed in the experimental studies utilized in this effort, the influence of the walls on NO oxidation rates is small. The effect would be additionally reduced in reactant systems for which the time to the NO_2 peak is relatively short (i.e., two hours or less).

- As we concluded earlier, we expect that the presence or absence of wall effects would result in no detectable differences in the rate of formation of HNO_3, largely because of the strong tendency of N_2O_5 to hydrolyze. Similarly, whether HNO_3 is formed in the gas phase, subsequently migrating to the wall, or whether it is formed directly on the wall, it is unlikely that the site of hydrolysis will have much of an effect on the observed chemistry. While nitric acid is commonly used as an oxidant when concentrated (60%) in the liquid phase [Godt, et al. (1956)], it is ineffective as an oxidant at low concentrations. The highest attainable concentration of HNO_3 during the chamber runs is a value that is numerically equal to the initial NO_x concentration, which never exceeded 4 ppm.

5. Conclusion

We conclude, based on the preceding discussion, that no significant amounts of NO and NO_2 are lost directly to the walls and that the loss of N_2O_5 and HNO_3 to the walls should not alter the observed photochemistry. However, it is not possible at this time to ascertain the degree to which the walls might accelerate the oxidation of NO. Wall effects, then, probably do not have to be taken into account in our validation efforts. Nonetheless, it is highly desirable that experimenters undertake to establish the magnitude of wall effects under a wide variety of experimental conditions, and that they do so in the near future. Until this is done, the possibility that such effects may be of consequence will remain an open issue.

E. Estimates of Experimental Error

Before comparing model predictions with experimental observations, it is desirable to establish both the accuracy and the precision of the measurements. Accuracy refers to the extent to which a given measurement agrees with the true but unknown value of the parameter being measured. Precision refers to the extent to which a given set of measurements agrees with the mean of the observations. Thus, if in a given experiment we observe y_i and the true and unknown value of the observed quantity is η_i, then we might state that

$$y_i = \eta_i + b_i + \varepsilon_i$$

where b_i is a bias that impinges upon the experiment and ε_i is a random error, which we will assume to be normally distributed with mean zero and variance σ^2 (or $\varepsilon(0, \sigma^2)$). If b_i is large relative to η_i, we say that y_i is *inaccurately* determined. If σ is large, with the result that ε_i is large, we say that y_i is *imprecisely* determined.

Inaccuracies in determination of concentrations are largely attributable to lack of specificity or accuracy in analytical procedures, particularly in the instrumentation used to monitor concentrations during the course of an experiment. Imprecision is detected through the poor repeatability of an experiment, the results of which may or may not be accurately determined. There may be a wide variety of causes of imprecision, some of which are also attributable to instrumentation problems.

1. The Accuracy of the Analytical Instruments

The four pollutant species of primary importance in our modeling efforts, NO_2 , NO , O_3 , and hydrocarbons, were all measured using standard instrumentation and techniques.

- Hydrocarbons were determined individually by gas chromatography; the accuracy of these measurements is estimated to be $\pm$ 10% at a concentration level of 1 ppm.

- Oxidants were measured using two independent techniques: the Mast Ozone Meter and neutral KI analysis. Corrections to KI readings were required to account for interferences due to PAN and NO_2 . Despite the corrections the KI measurements exceeded the Mast readings by an average of 50%. As Dr. S.L. Kopczynski of the Division of Chemistry and Physics is of the opinion that the KI technique is the more accurate of the two procedures, we have validated our model using the results of the KI analyses.

- Oxides of nitrogen were sampled manually into fritted bubblers containing Saltzman reagent. Nitric oxide was oxidized to form NO_2 by reaction with sodium dichromate. Dr. Kopczynski has estimated that this conversion is almost 100% efficient. Absorbance was read on a Beckman DU spectrometer reading 2 ppm at full scale.

In general, the accuracy of these various measurements is a function of the concentration level of the pollutant being measured. Accuracy is poorest over the low concentration range. As most pollutants are present at low concentrations at some time during the course of a reaction, questions of accuracy will inevitably arise with regard to chamber studies. For example, at concentrations of NO_2 below 0.15 ppm, concentrations can be determined no more accurately than $\pm$ 50%. At the higher concentrations encountered as the reaction proceeds, the accuracy of the readings improves substantially. Unfortunately, no recalibration of the oxidant or the nitrogen oxide analyzers was performed during the ten-month study.

2. The Repeatability of Experimental Runs

Because replicate runs were made for the toluene-NO_x system at five different sets of initial conditions and for the toluene-n-butane-NO_x system at three sets of initial conditions, we have been able to estimate the precision of the hydrocarbon, NO , and NO_2 measurements in those systems by calculating pooled standard deviations [Hunter (1960)].

The equations used to calculate the pooled standard deviation, s_p , are as follows:

$$s_j^2 = \frac{\sum_{i=1}^{N_j} (y_i - \bar{y})^2}{N_j - 1}$$

and

$$s_p^2 = \frac{\sum_j (N_j - 1) s_j^2}{\sum_j (N_j - 1)}$$

where N_j is the number of observations made at time t , j is the index representing a given set of replicates, y_i are the observed concentrations at time t , and $\bar{y}$ is the average of the observations made at time t . The pooled standard deviation is then simply the square root of the pooled variance s_p^2 . The error bounds calculated at the 90% confidence level ($\pm t_{\nu,0.90} s_p$) are listed in Table 4 for the specific times indicated. Bounds may be indicated graphically by shading the regions of uncertainty. In Figures 1 and 6, we display the uncertainty bounds for the toluene-NO_x and the toluene-n-butane-NO_x validations respectively.

Our impression of the chamber data is that, in spite of the lack of recalibration of the light intensity and chemical analyzers, the data are in general reproducible, were carefully taken, and are as suitable as any currently available for validation purposes. Although the data were taken in 1966 and 1967, at a time prior to the development of photochemical kinetic mechanisms for atmospheric reactions, the investigators did exercise sufficient care in quantifying those parameters important in validation of these models.

TABLE 4. Precision Bounds (90% Confidence Levels) for Toluene-NO_x and Toluene-n-Butane-NO_x Data

TIME (MINUTES)	SPECIES	ν**	s_p†	UNCERTAINTY BOUND AT 90% CONFIDENCE*
SYSTEM: TOLUENE-NO_x				
80	NO_2	5	0.76	±.15 ppm
160	NO_2	4	0.94	±.21
240	NO_2	3	0.16	±.37
320	NO_2	2	0.07	±.21
50	NO	5	0.07	±.13
100	NO	3	0.11	±.26
80	HC	4	0.24	±.50
160	HC	4	0.23	±.49
240	HC	4	0.22	±.48
320	HC	4	0.18	±.37
SYSTEM: TOLUENE-n-BUTANE-NO_x				
80	NO_2	3	0.14	±.34 ppm
160	NO_2	3	0.12	±.28
240	NO_2	3	0.07	±.17
320	NO_2	3	0.02	±.04
50	NO	3	0.03	±.07
80	HC	3	0.22	±.53
160	HC	3	0.17	±.40
240	HC	3	0.21	±.50
320	HC	3	0.16	±.37

* Calculated as $\pm t_{\nu,0.90} s_p$, where $t_{\nu,0.90}$ is the Student t statistic with ν degrees of freedom

** Degrees of freedom

† Pooled standard deviation

For example, dilution rates and the rate of conversion of NO to NO_2 in the absence of hydrocarbons were measured for all reactant systems. Probably the greatest weakness in the chamber data with regard to their use in validation is the lack of precise knowledge of the light intensity. As will be shown in Section IV the magnitude of light intensity has a substantial effect upon the time to the NO_2 peak predicted by the model.

IV. VALIDATION OF THE MECHANISM

Validation of the kinetic mechanism consists in

- obtaining estimates of the various parameters in the mechanism -- the reaction rate constants and the generalized stoichiometric coefficients -- and establishing, when appropriate, how these parameters vary with changes in the species and composition of hydrocarbons in the reactant mixture

- carrying out sensitivity studies for these parameters, i.e., establishing the effect of controlled variations in the magnitudes of the various parameters on the concentration/time profiles for NO, NO_2, O_3 and hydrocarbon

- generating concentration/time profiles for the various reactant mixtures using specified initial conditions. These predictions are then compared with experimental results to assess the "goodness of fit".

In the first part of this section, we discuss the basis for selection of some of the more uncertain parameters, notably the rate constants for the hydrocarbon oxidation reactions (with O, O_3, and OH) and the generalized stoichiometric coefficients α, β, γ, and ε. In the second portion of the section, we present the validation results for each of the four hydrocarbon systems studied. Results are summarized as a series of plots displaying both predicted and measured concentrations. We would remind the reader that the results reported represent the second validation effort involving the present model. Previous validation studies are described in detail in Seinfeld, et al. (1971).

A. Estimation of Parameters

1. The Rate Constants

While the kinetic mechanism is both general and compact, we have striven to formulate it in such a way that the majority of rate constants may be taken from the literature dealing with the study of individual reaction steps. However, due to the generalized nature of the model, some rate constants, of necessity, are artifacts, notably those specified for reactions 6, 11, 12, 13, and 15. All other rate constants have been estimated from the results of experiments reported in the literature; their magnitudes and sources are given in Seinfeld, et al. (1971).

As described in Section II, k_6 was selected such that a model based on four differential equations, with HNO_2 in steady state, gave predictions comparable with those of a model in which a differential equation for HNO_2 was included. In the remainder of this section we discuss the basis for estimating the four remaining rate constants, k_{11}, k_{12},

k_{13} , and k_{15} , those associated with the hydrocarbon oxidation reactions and the RO_2-NO_2 reaction.

The results of early validation runs indicated that the literature values of k_{11} (O + HC) , as given by Johnston, et al. (1970), are too low to account for the observed early oxidation rate of hydrocarbons and the oxidation of NO to NO_2 . A number of reactions were excluded from the mechanism for the sake of compactness, notably the oxidation of hydrocarbons by alkyl, oxy, and peroxy radicals. The omission of one or more of these "reactions of lesser importance" might account for the apparent "smallness" of k_{11} . While the hydrocarbon-radical reactions cited do not, in general, result in a rapid increase in the number of free radicals, the radicals produced may be of higher reactivity than those present originally. The overall reactivity of the smog system may thus increase with time.

As an example, consider hydrogen abstraction from n-butane by a peroxymethyl radical.

$$CH_3OO\cdot + CH_3CH_2CH_2CH_3 \rightarrow CH_3OOH + CH_3CH_2\dot{C}HCH_3$$

(This type of reaction is discussed by Leighton (1960), p. 217.) One hydrocarbon molecule is consumed in this reaction, and a 2-butyl radical is formed in exchange for the peroxymethyl radical. Several reactions now become likely. First, the 2-butyl radical may react with oxygen to form a hydroperoxyl radical and an olefin.

$$CH_3CH_2\dot{C}HCH_3 + O_2 \rightarrow CH_3CH{=}CHCH_3 + HO_2$$

$$\text{or} \quad CH_3CH_2CH{=}CH_2 + HO_2$$

This reaction is of interest because a low reactivity paraffin is replaced in the system by a highly reactive olefin, which then participates in further chain propagation reactions. In addition the hydroperoxide formed when the peroxymethyl radical reacts with butane photolyzes readily, leading to still further chain branching.

$$CH_3OOH + h\nu \rightarrow CH_3O\cdot + \cdot OH$$

The overall result of the peroxymethyl oxidation, then, if it in fact occurs to a significant degree, is the formation of an olefin and three free radicals.

The reactions between hydrocarbons and alkyl, oxy, and peroxy radicals, although not thought to be particularly rapid, probably still play an important role early in the smog forming process because 1) they compete with O atom attack on hydrocarbons, a reaction which itself is not very fast due to the low O concentration and 2) the concentration of radicals increases rapidly until the steady-state level is achieved. However, these reactions are not included in the mechanism because there is a dearth of kinetic data for the radical-hydrocarbon reactions and because knowledge of the magnitude of the radical populations is lacking. Consequently, values of k_{11} higher than those reported in the literature have been adopted to account for the early loss rate of hydrocarbon observed experimentally. We note, however, that the influence of other reactions, such as the OH-hydrocarbon reaction, become relatively greater as the smog reactions proceed. The contribution of the radical-hydrocarbon reaction to the overall hydrocarbon loss rate thus becomes less significant with time.

In the future it will be desirable to investigate the possibility of adding a radical-hydrocarbon reaction to the mechanism to account for the rapid early loss rate of hydrocarbon and NO observed. It might also be possible to employ literature values of k_{11} by modifying the values of the stoichiometric coefficients, thus avoiding the addition of other reactions. These possibilities will be explored in the near future when an extensive sensitivity analysis of the model is completed.

In general, we were able to use literature values for k_{12} and k_{13}, the rate constants for the OH and O_3 hydrocarbon oxidation reactions, for the validation runs [Johnston, H.S., et al. (1970); Morris, E.D., Jr., et al. (1971)]. In cases where O_3 does not react directly with the hydrocarbon, a small residual value of k_{13} has been assigned to account for the reaction of ozone with hydrocarbon oxidation products. For example, in the case of n-butane, it is possible that various butenes form subsequent to O or OH attack on the hydrocarbon. The reaction of these butenes with O_3 is accounted for through the artificial increase in k_{13}.

Finally, the value of k_{15} was selected so that, on a qualitative basis, the predicted concentration/time profiles of organic nitrates and pernitrates formed as reaction products conformed with expected behavior. The observed rate of loss of NO_2 after the NO_2 peak was also taken into account in estimating the magnitude of this constant.

2. Generalized Stoichiometric Coefficients

Stoichiometric coefficients are those parameters introduced into each individual reaction step to satisfy the requirement of conservation of mass. While these coefficients, in general, are easily established by carrying out a mass balance for all elements appearing in the reaction expression, a problem arises in the treatment of vaguely defined species such as the generalized hydrocarbon, HC. We cannot specify the exact number of atoms that comprise this fictitious species, and thus it is impossible to derive or compute appropriate coefficients. To skirt this problem, we introduce flexible parameters, termed "generalized" stoichiometric coefficients, such as α in the reaction, $HC + O \rightarrow \alpha RO_2$. These generalized coefficients must be established through deductive procedures such as "chemical" arguments and trial and error calculations. In the discussion that follows, we present the rationale for selecting the generalized coefficients, α, β, γ, and ε introduced in the new mechanism. See Seinfeld, et al. (1971) for an earlier discussion of this same topic.

We first consider the selection of a value of α, the number of radicals formed in the reaction of hydrocarbons and atomic oxygen. This choice is of prime importance, as α strongly governs the chain length of the reaction, and the hydrocarbon-atomic oxygen reaction itself is critical in determining the rate of oxidation of NO to NO_2. As we mentioned in Section II, in earlier validation studies we have treated this parameter as a function of the NO/HC ratio over the course of the reaction, rather than as a constant. However, we have considered the need for a functional relationship between α and NO/HC to be a weakness in the formulation. We have found in the current validation studies that α could indeed be taken as a constant for a particular hydrocarbon and we have done so throughout. We attribute the earlier need for a variable α to weaknesses in the data base used at that time. Unfortunately, we have not as yet discovered a procedure for obtaining a priori estimates of α. Values of α used in validation were established by comparison of predicted and observed concentrations of NO and hydrocarbon.

The stoichiometric coefficient γ is determined by comparing predicted and observed concentrations of a reaction system in which an olefin is the principal reacting hydrocarbon. The magnitude of the coefficient is selected so as to minimize discrepancies between the predicted and observed hydrocarbon loss rate after the NO_2 peak and between the maximum predicted and observed ozone levels ultimately attained. An olefin reaction is desirable because ozone

reacts directly and rapidly with hydrocarbons of this class. This reactant system will thus give a good indication of the effect of the O_3-HC reaction on the NO_2 decay curves. Because most three carbon and greater hydrocarbons can form olefins as degradation products, the value of γ is the same for all hydrocarbon systems.

The stoichiometric coefficient β in reaction 12 is analogous to α and γ, in that it governs the number of $RO_2^\cdot$ radicals formed due to reaction of hydrocarbons -- in this instance, with hydroxyl radicals. As in the case of the other generalized stoichiometric coefficients, β is treated as a constant for a given hydrocarbon system. In general we expect that β will be about one, since likely products of the HC-OH$\cdot$ reaction are one free radical and an aldehyde (in the case of olefins) or water (in the case of paraffins). Accurate estimation of ε, the number of moles of OH formed per mole of RO_2 that reacts with NO, is important in simulation of the effect of CO.

In order to estimate ε, along with β, we require experimental data for reaction systems in which the initial charge of CO varies from zero to some substantial concentration, for the product of β and ε will to a large degree determine the amount by which the time to the NO_2 peak is shortened for a given increase in CO concentration. This point can be seen by inspection of the algebraic steady state equation for the $RO_2\cdot$ radical, given in Seinfeld, et al., p. B-18 (1971). In particular, note that in this equation the $RO_2^\cdot$ concentration is inversely proportional to

$$(1 - \beta\varepsilon)\ k_{12}k_{14}(HC)(NO) + k_{12}k_{15}(HC)(NO_2)$$

Since NO is oxidized by both $HO_2^\cdot$ (formed in reaction 8) and $RO_2^\cdot$, changes in the product $\beta\varepsilon$ will affect the concentration of the $RO_2^\cdot$ radicals and consequently the relative contribution of $RO_2^\cdot$ to the total NO oxidation rate. Thus, for a fixed value of $\beta\varepsilon$, the time to the NO_2 peak will decrease as the initial CO concentration increases, because the NO loss rate will become more negative. Ir general observed reductions in time to the NO_2 peak are greatest in the presence of CO when the hydrocarbon components of the system are of low reactivity and least when reactant systems consist primarily of highly reactive olefins [Dodge, et al. (1972)].

In addition to making these qualitative observations, we can also specify quantitative limits for the product $\beta\varepsilon$. Since OH$\cdot$ attacks both HC and CO and since the products of both reactions are radical species capable of oxidizing

NO to NO_2 ($RO_2\cdot$ in the former case and $HO_2\cdot$ in the latter), it is necessary that the number of $HO_2\cdot$ radicals formed in the CO-OH· reaction (always equal to one) be greater than the number of $RO_2\cdot$ radicals formed in the HC-OH· reaction in the presence of CO . If the product $\beta\varepsilon$ were greater than one, CO would effectively inhibit the rate of NO oxidation. This effect would be attributable to the scavenging of OH· radicals by CO , thereby diminishing the supply of OH· available for possible reaction with HC , a reaction capable of generating more radicals than the single $HO_2\cdot$ produced in the CO-OH· reaction. This point can also be verified by inspection of equation B-2b in Seinfeld, et al. (1971). If $\beta\varepsilon > 1$, the negative terms $(1 - \beta\varepsilon)$ in the denominator become positive, $d(NO)/dt$ is then also positive, and NO is not converted to NO_2 . Thus, we require that $\beta\varepsilon < 1$. Finally, the value of ε must be less than one, as all $RO_2\cdot$ are actually $HO_2\cdot$ if ε is equal to one.

A final consideration in the selection of the value of β is that the magnitude of this coefficient strongly influences the NO decay and hydrocarbon consumption rates in the vicinity of $(NO) = 1/2(NO)_o$. During that time reaction 12 is the most important factor in the loss of HC and NO . Thus the shapes of the HC and NO decay curves in that region depend upon the proper choice of β .

3. Sensitivity of the Model to Variations in the Magnitudes of Parameters

We have carried out a large number of validation runs during both this study and that reported in Seinfeld, et al. (1971). Many of these runs involved the investigation of the effect of varying the magnitude of a parameter on the predicted concentration/time profile. These efforts can thus be viewed, in part, as an informal sensitivity study of the current version of the kinetic mechanism. Through the experience gained, we have acquired a fairly good "feeling" for the extent to which variations in the rate constants, stoichiometric coefficients and initial conditions alter the predicted concentration profiles. However, we have not as yet carried out a formal sensitivity analysis. It is anticipated that we will undertake such a study for EPA as a part of our efforts under contract 68-02-0580.

In place of the full and formal study that we have suggested is eventually needed, we carried out a more limited investigation of model sensitivity. We examined the effect of variations in four parameters -- k_1 (light intensity)* ,

---

*The uncertain variable in the reaction of interest is noted in parentheses.

k_6 (water concentration) , k_7 (light intensity) , and initial NO_2 concentration $(NO_2)_o$--on predicted time to the NO_2 peak, T . These parameters have been identified in previous studies as being the parameters whose variations would likely have a substantial influence on predictions. The variable T was selected as the decision variable because it had been observed previously that it is particularly sensitive to variations in the parameters cited, because other key variables such as time to the onset of O_3 formation are closely linked to it, and because it can be conveniently expressed as a scalar.

The sensitivity calculations were performed for the toluene-n-butane system for various initial concentrations. The four parameters were varied within the limits of their estimated uncertainty bounds and the effects of these changes on T were noted. Typical results are presented in Table 5. The mechanism is clearly quite sensitive to variations in the NO_2 photolysis rate and initial NO_2 concentrations, but is insensitive to variations in HNO_2 production and photolysis rates. Unfortunately, both k_1 and $NO_2|_o$ are subject to considerable experimental uncertainty.

In carrying out the validation runs that are reported in the following section, we calculated concentration/time profiles using, first, base values of all parameters and, second, base values of the parameters with k_1 and $NO_2|_o$ varied within their limits of uncertainty so as to minimize the discrepancy between prediction and experiment. In this way one can compare the paired results and "get a feeling" for the degree of variation (really, improvement) in predicted values to be expected as a result of parameter variation for the limited, yet perhaps highly indicative, case of varying two "sensitive" parameters. Viewed another way, we demonstrate how lack of accuracy in certain measurements, in this case initial NO_2 concentration and light intensity, can affect predictions, and thus our ability to properly assess the validity of the mechanism.

TABLE 5. Sensitivity of the Model to Light Intensity, Water Concentration, and Initial NO_2 Concentration

Base Values of Parameters:

$NO_2\|_o$	=	0.07 ppm
$NO\|_o$	=	1.10 ppm
hydrocarbon (toluene + n-butane)	=	4.62 ppm
k_1	=	.266 min^{-1}
k_6	=	$5x10^{-4}$ $ppm^{-1}min^{-1}$
k_7	=	$5x10^{-3}$ min^{-1}

NO_2 peak occurs at 112 minutes for these settings of the base parameters

Variation in Parameter	Resultant Change in Time to NO_2 peak (minutes)
k_1 - 0.10	+57
k_1 + 0.10	-28
k_6 - 25%	+ 4
k_6 + 25%	- 4
k_7 - 50%	0
k_7 + 50%	0
$NO_2\|_o$ - 50%	+21
$NO_2\|_o$ + 50%	-12

B. The Validation Results

In this section we present validation results for the mechanism shown in Table 1 for the following reactant systems:

Reactant System	Number of Sets of Experimental Data
toluene-NO_x	5
toluene-n-butane-NO_x	3
propylene-(ethane)-NO_x	4
auto exhaust	2
	14

As we have discussed, for each set of data we carried out a validation using base values of the parameters and a validation using base values of all parameters except k_1 and $NO_2|_o$, which were varied within their limits of uncertainty to obtain improved (but not necessarily optimal) predictions. We thus report the results of two computer simulations for each data set, "mean value" predictions and "improved" predictions. These pairs are labeled using the same figure number, with an "A" designating the "improved" concentration profiles. Figure numbers, EPA experiment identification number, initial conditions, dilution rates, and variations in k_1 and $NO_2|_o$ are given in the List of Figures, Table 6. A key to reading the figures is given in Table 7.

In carrying out the simulations in which parameters were varied from their base values, no attempt was made to minimize the discrepancy between prediction and experiment. A qualitative, "experience-based" judgment was made as to what variations in k_1 and $NO_2|_o$, within their limits of uncertainty [$k_1 = 0.266 \pm 0.10$ min^{-1}, $NO_2|_o \pm 50\%$], would reduce the discrepancy, and the "improved" simulation was carried out. We do believe, however, that these results are of value in assessing the suitability of the mechanism for describing the chemistry. Yet it is likely that still greater improvements in fit could have been obtained if other parameters (rate constants, stoichiometric coefficients, and/or initial conditions) were also varied within their uncertainty limits. We did not feel, however, that in light of the uncertainties *in the experimental results* such simulations were warranted. Optimization studies are of interest at a time when more precise experimental data become available.

1. Toluene-NO_x Validations

Validation runs for the toluene-NO_x experiments were performed using the rate constants listed in Table 8. Note

TABLE 6. List of Figures

FIGURE	EPA NO.	HC TYPE	$(NO_2)_o$*	$(NO)_o$*	$(HC)_o$*	k_1†	AVG. DIL. RATE††
1	300	Toluene	.02	1.25	3.22	.266	5.50
1A	300	Toluene	.02	1.25	3.22	.216	5.50
2	258	Toluene	.05	.35	2.88	.266	4.63
2A	258	Toluene	.075	.35	2.88	.200	4.63
3	250	Toluene	.04	1.17	1.53	.266	5.48
3A	250	Toluene	.04	1.17	1.53	.200	5.48
4	272	Toluene	.04	.55	1.67	.266	5.40
4A	272	Toluene	.06	.55	1.67	.300	5.40
5	271	Toluene	.05	.32	1.20	.266	5.74
5A	271	Toluene	.075	.32	1.20	.366	5.74
6	251	n-Butane Toluene	.07	1.10	4.62	.266	5.85
6A	251	n-Butane Toluene	.035	1.10	4.62	.166	5.85
7	253	n-Butane Toluene	.08	.53	4.91	.266	5.90
7A	253	n-Butane Toluene	.04	.53	4.91	.266	5.90
8	257	n-Butane Toluene	.07	.27	4.26	.266	4.65
8A	257	n-Butane Toluene	.07	.27	4.26	.366	4.65
9	318	Propylene	.06	1.12	.51	.266	5.75
9A	318	Propylene	.06	1.12	.51	.166	5.75
10	325	Propylene	.04	.35	.45	.266	6.95
10A	325	Propylene	.04	.35	.45	.366	6.95
11	321	Propylene	.10	1.31	.275	.266	7.13
11A	321	Propylene	.05	1.31	.275	.266	7.13
12	329	Propylene	.05	.26	.24	.266	6.85
12A	329	Propylene	.075	.26	.24	.366	6.85
13	222	Auto Exhaust	.12	1.95	2.21‡	.166	5.37
14	231	Auto Exhaust	.23	2.80	.59‡‡	.266	5.75

* Units of ppm
† Units of minutes^{-1}
†† Units of liters minutes^{-1}

‡ $HC_1 = 1.15$, $HC_2 = 1.06$
‡‡ $HC_1 = 0.20$, $HC_2 = 0.39$

TABLE 7. Key to Figures

EXPERIMENTAL RESULTS:

NO

NO_2

OXIDANT

HYDROCARBON

PREDICTIONS:

NUMBERED FIGURES ARE CALCULATED USING MEAN VALUE OF k_1 AND INDICATED INITIAL CONCENTRATION OF NO_2 .

NUMBERED "A" FIGURES ARE IMPROVED PREDICTIONS BASED ON CHOICES OF k_1 , AND/OR $(NO_2)_o$ AS INDICATED IN THE LIST OF FIGURES.

SHADED REGIONS INDICATE PRECISION BOUNDS BASED UPON POOLED STANDARD DEVIATION AT 90% CONFIDENCE LEVEL.

that the value of k_{11} adopted is about sixty times greater than the literature value of the constant. This substantially elevated value was required if discrepancies between hydrocarbon and NO predicted and experimental values were to be acceptably small during the early portion of the experimental run. (See Section III for a more detailed justification of this assumption.) The value of k_{12} is an estimate based on measurements made by Morris, E.D., Jr., et al. (1971) for the xylene-OH reaction. A value of k_{13} was adopted that is less than that employed by us for n-butane in previous validation studies. This decrease in k_{13} takes into account the fact that aromatics typically react to form acetylenes as oxidation products in preference to olefins. Thus, the use of this reduced value permits more accurate description of the post-NO_2-peak hydrocarbon oxidation.

Turning now to the stoichiometric coefficients, the value of α selected was based on the rate of loss of NO observed early in the irradiation. Because toluene and n-butane are both low reactivity hydrocarbons, carbon monoxide might be expected to affect the toluene-NO_x system in a manner similar to the n-butane-NO_x system. Consequently, β and ε were given the same value for toluene as they were for n-butane, as reported in Seinfeld, et al. (1971). The value of γ is the same as that used for the propylene system, which will be discussed shortly.

Plots of predicted and experimental values of concentrations with time are shown in Figures 1 through 5; improved predictions, obtained by varying either k_1 or $(NO_2)_o$, or both, are given in Figures 1A through 5A.

2. Toluene-n-Butane-NO_x Validations

As toluene and n-butane are hydrocarbons having similar reactivities, a mixture of these species will remain in approximately constant proportion throughout the course of a reaction. We thus elected to combine the two species, for modeling purposes, into a single "lumped" hydrocarbon. The rate constants and stoichiometric coefficients for this "lumped" species were estimated by computing the weighted average of the constants for the individual species, the weights being the initial mole fraction of each hydrocarbon. Because the ratio of toluene to n-butane remained approximately constant throughout the course of the reaction, it was not necessary to update the rate constants during the integration. Rate constants and stoichiometric coefficients for this system are listed in Table 9.

As in the case of toluene, the value of the O-n-butane rate constant was taken to be sixty times greater than the literature value. The literature value for the OH-n-butane

TABLE 8. Validation Parameters for Toluene-NO_x Experiments

Rate Constants

k_1	0.266	min^{-1}
k_2	2.76×10^6	min^{-1}
k_3	21.8	$ppm^{-1}min^{-1}$
k_4	0.006	$ppm^{-1}min^{-1}$
k_5	0.1	$ppm^{-1}min^{-1}$
k_6	5.0×10^{-4}	$ppm^{-1}min^{-1}$
k_7	5.0×10^{-3}	min^{-1}
k_8	-	
k_9	1.8×10^3	$ppm^{-1}min^{-1}$
k_{10}	10.0	$ppm^{-1}min^{-1}$
k_{11}	6.0×10^3	$ppm^{-1}min^{-1}$
k_{12}	1.5×10^4	$ppm^{-1}min^{-1}$
k_{13}	7.5×10^{-5}	$ppm^{-1}min^{-1}$
k_{14}	1.8×10^3	$ppm^{-1}min^{-1}$
k_{15}	30.0	$ppm^{-1}min^{-1}$

Stoichiometric Coefficients

α	6.0
β	1.2
γ	4.0
ϵ	0.61

FIGURE 1. EXPERIMENT #300. TOLUENE.

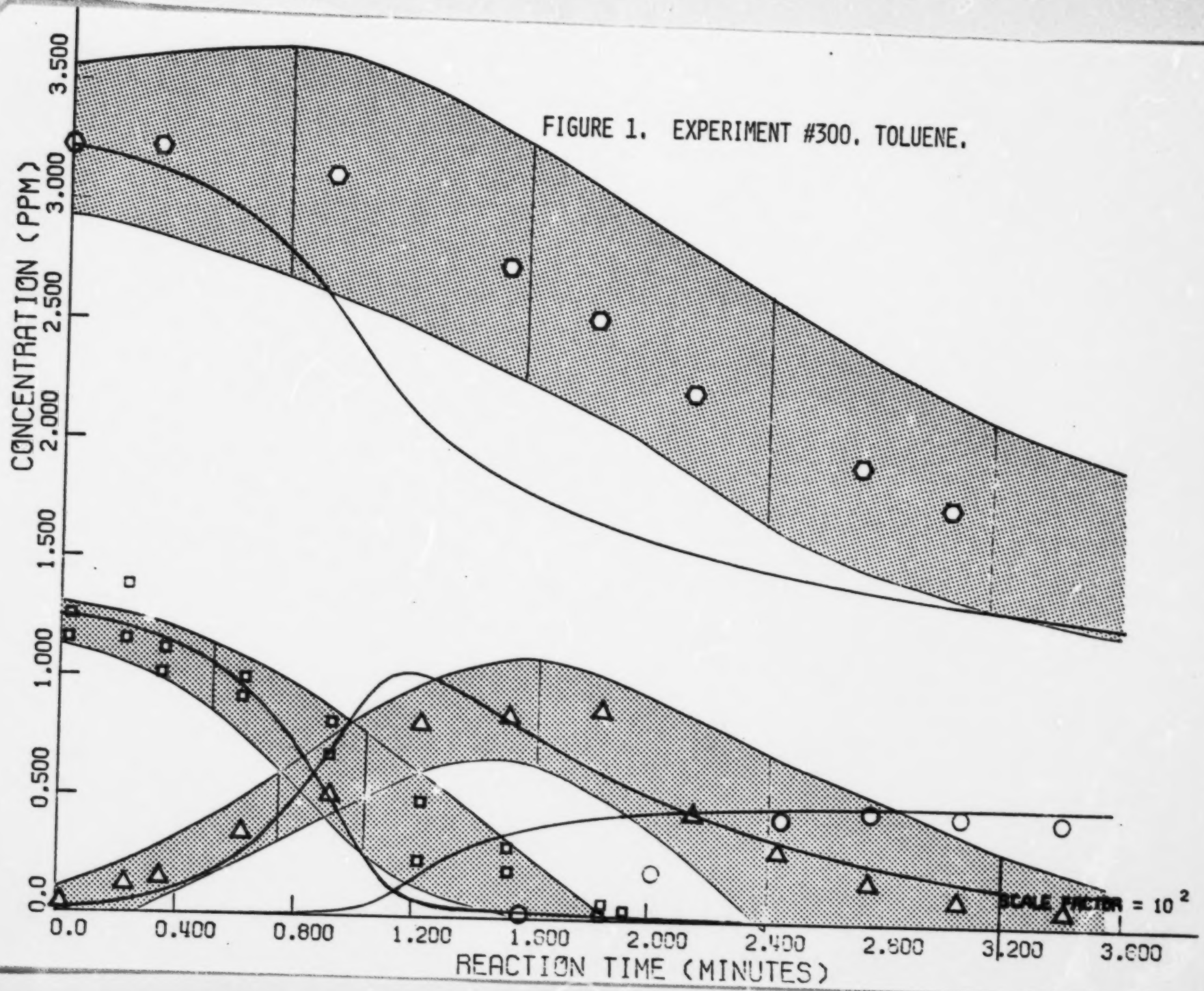

FIGURE 1A. EXPERIMENT #300. TOLUENE.

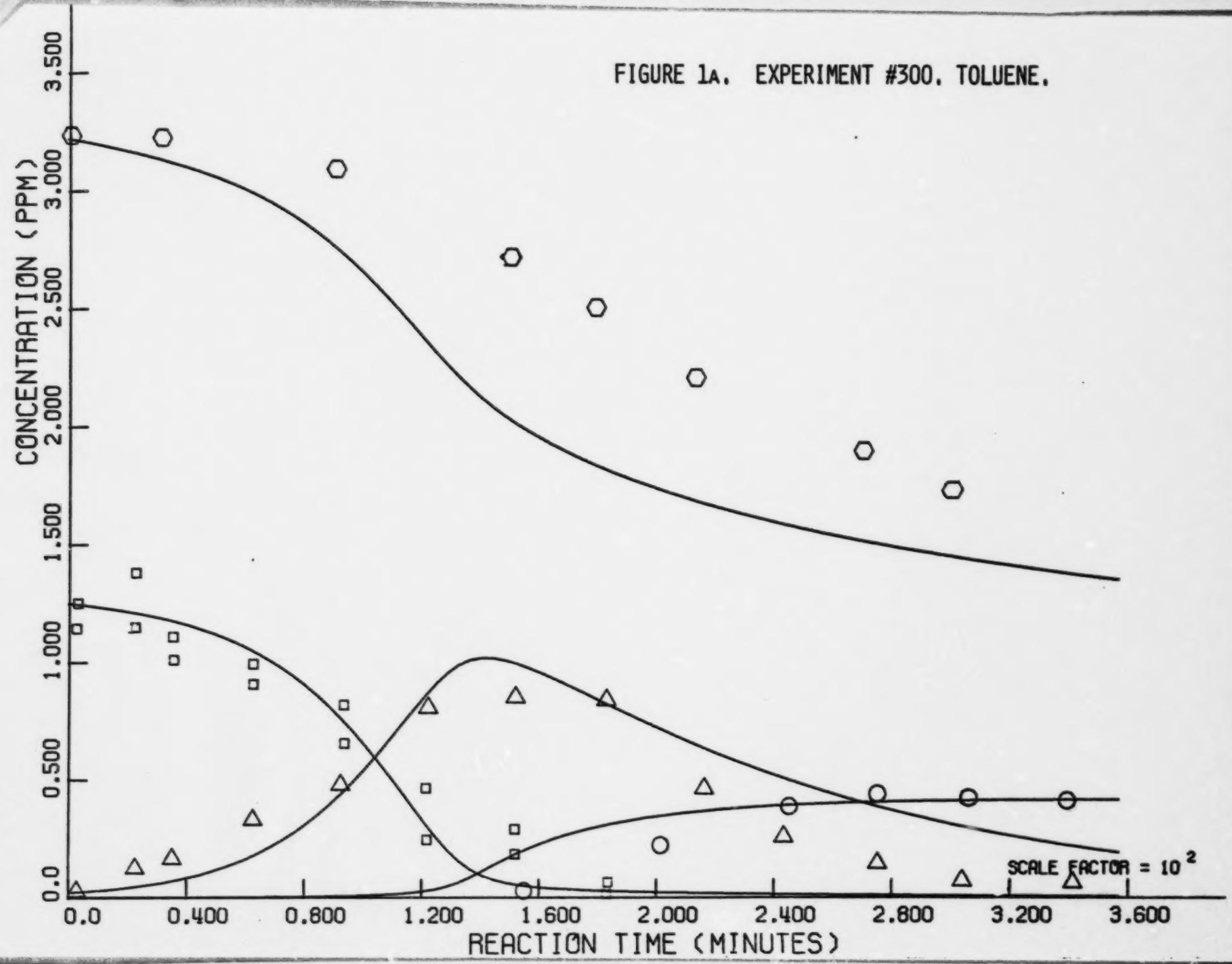

FIGURE 2. EXPERIMENT #258. TOLUENE.

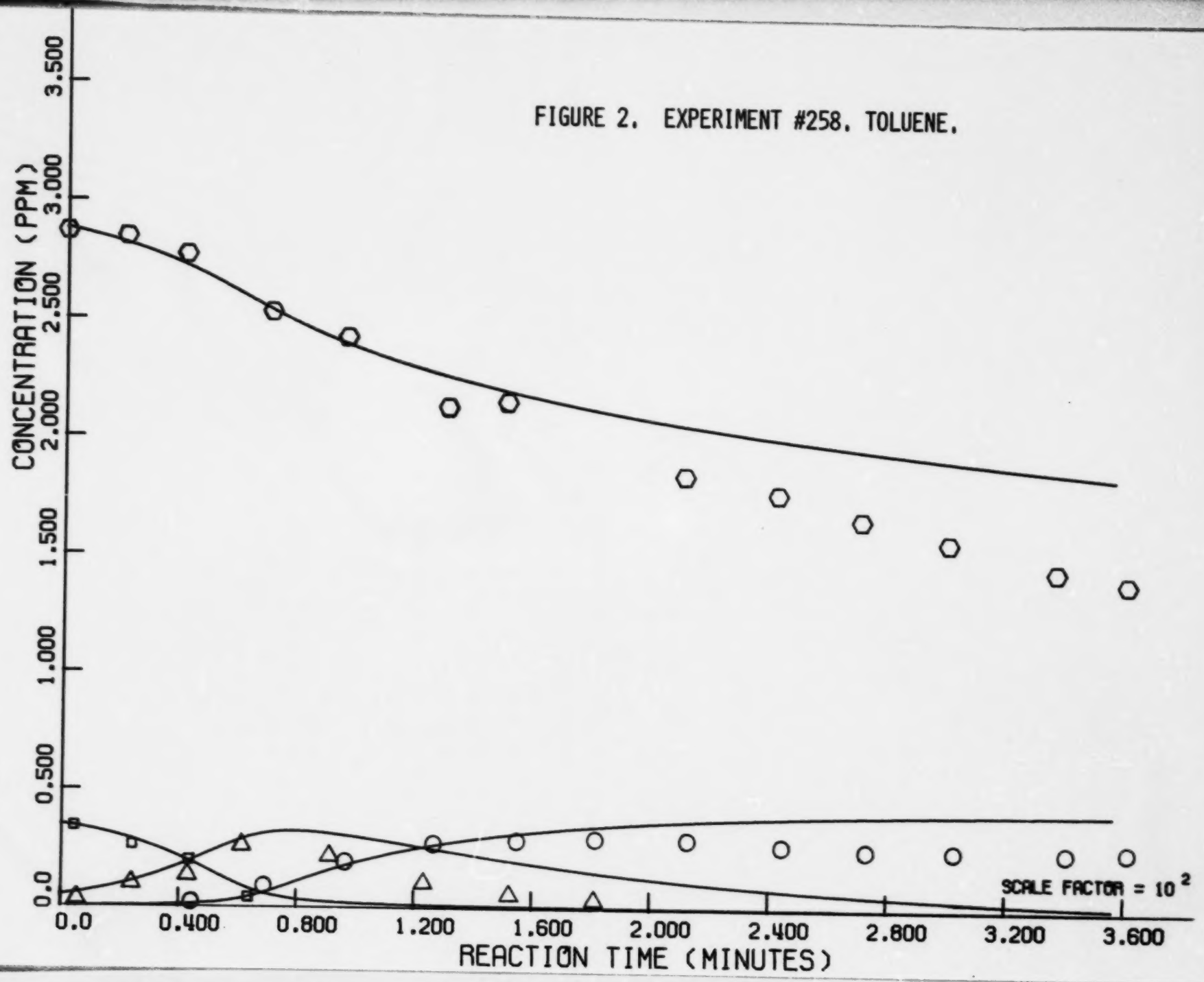

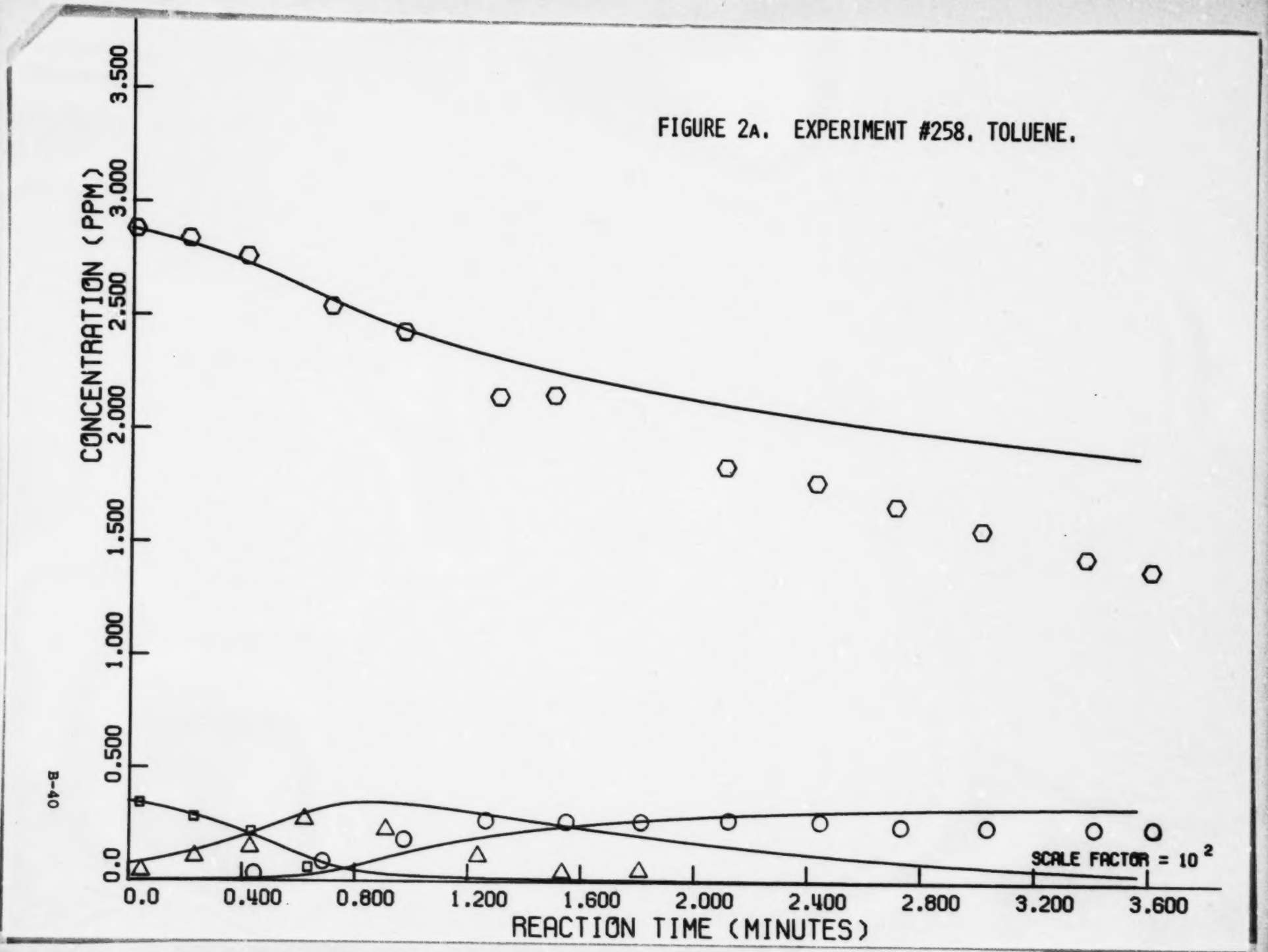
FIGURE 2A. EXPERIMENT #258. TOLUENE.
CONCENTRATION (PPM)
0.0
0.500
1.000
1.500
2.000
2.500
3.000
3.500
0.0
0.400
0.800
1.200
1.600
2.000
2.400
2.800
3.200
3.600
REACTION TIME (MINUTES)
SCALE FACTOR = 10 2

FIGURE 3. EXPERIMENT #250. TOLUENE.

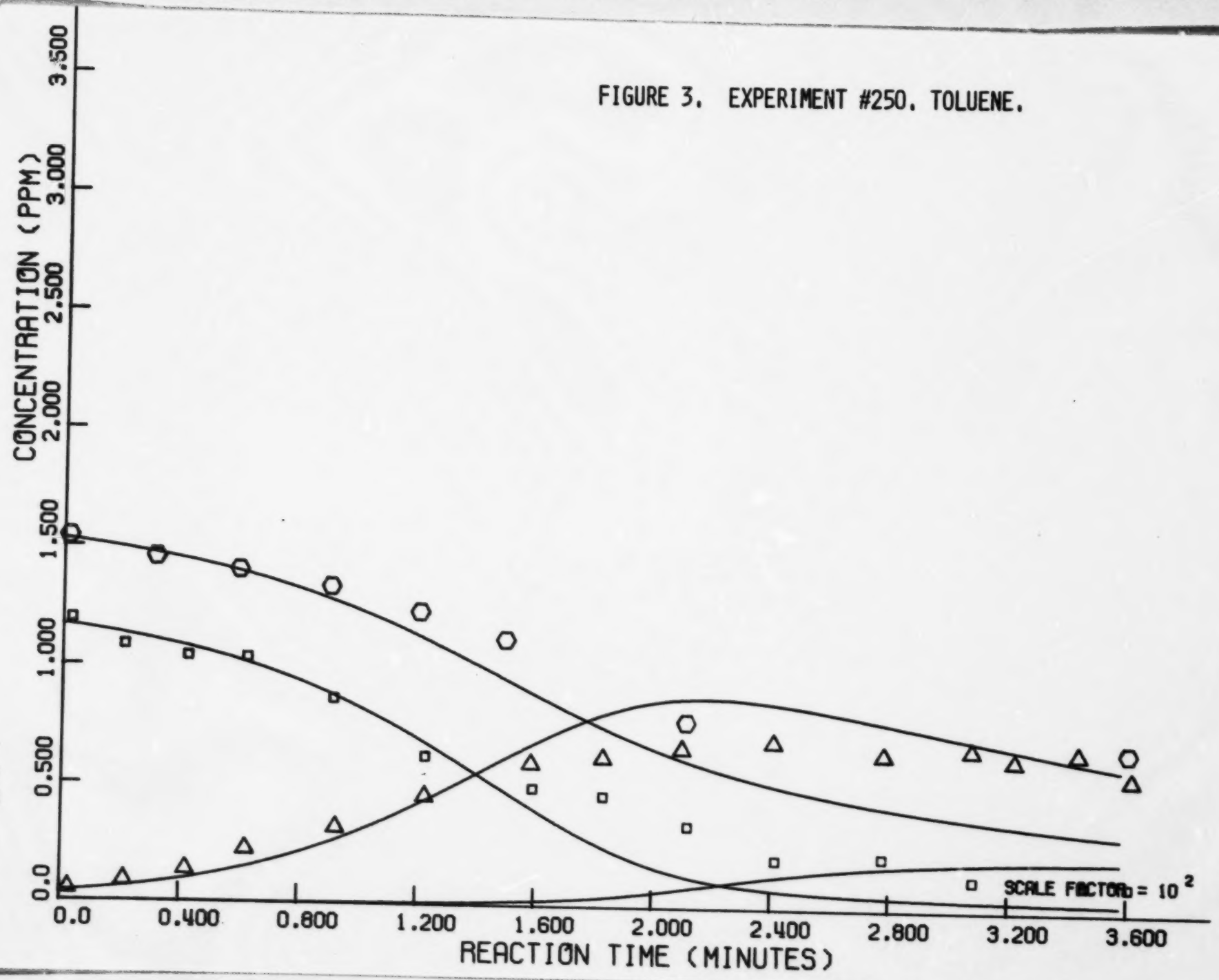

FIGURE 3A. EXPERIMENT #250. TOLUENE.

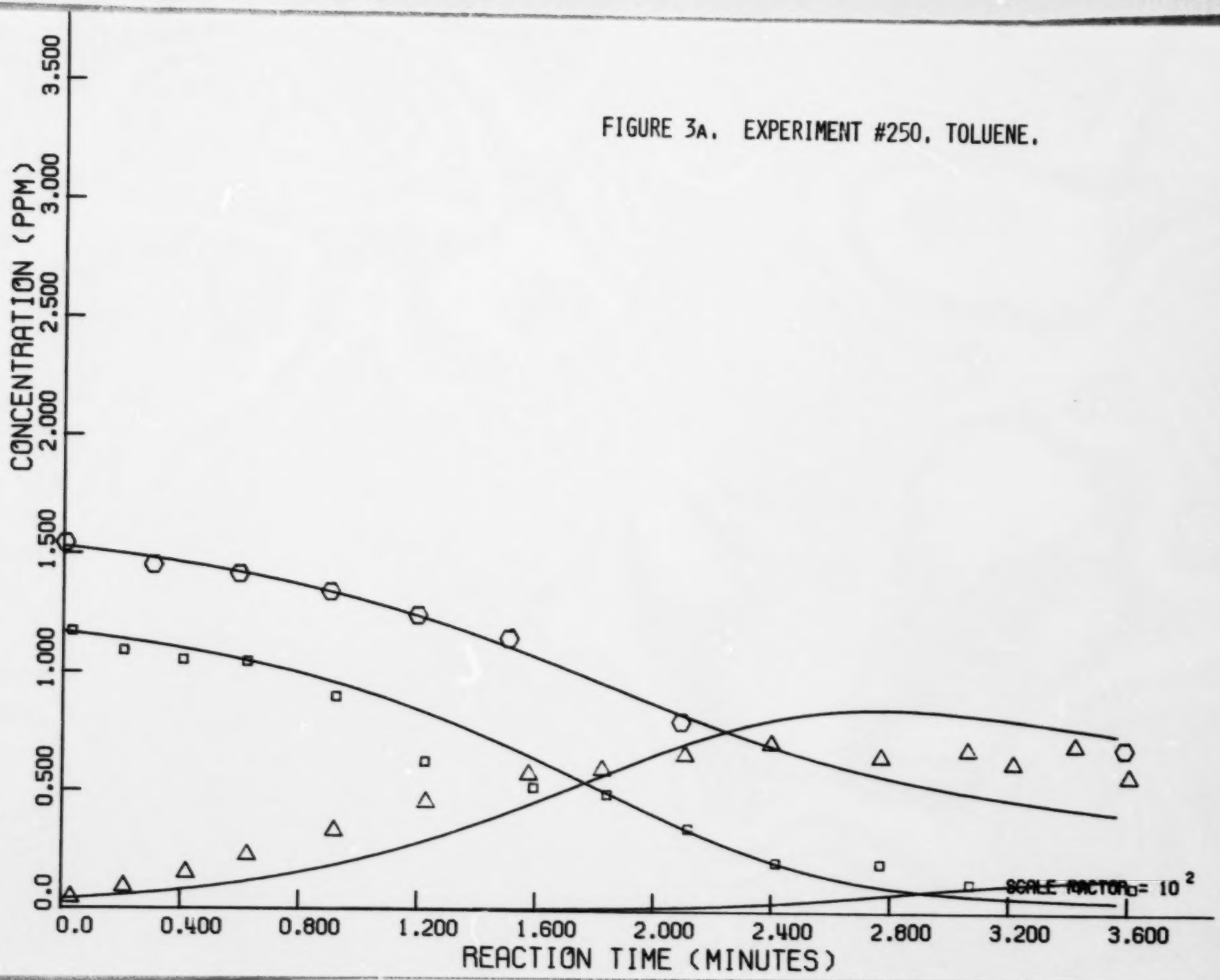

FIGURE 4. EXPERIMENT #272. TOLUENE.

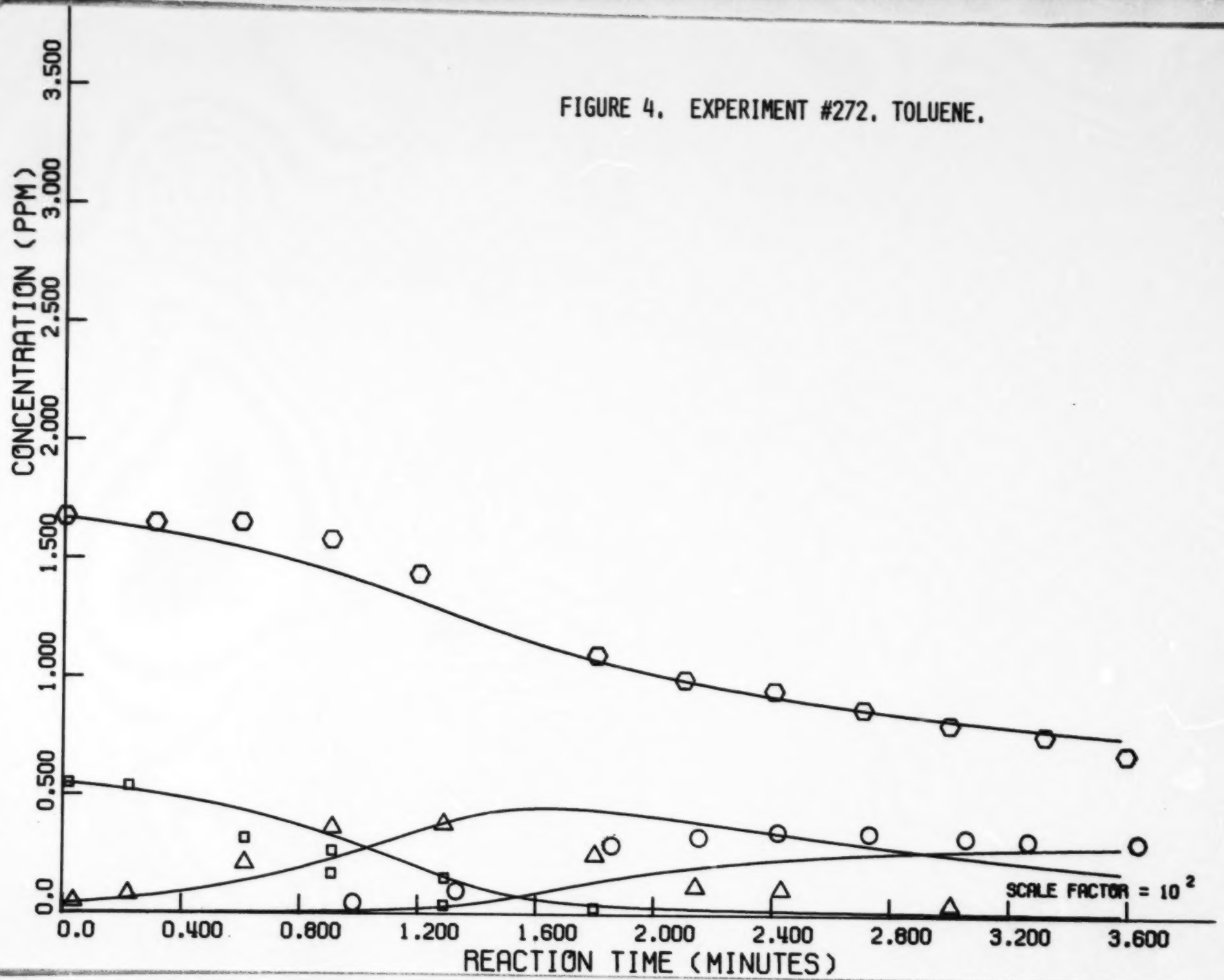

FIGURE 4A. EXPERIMENT #272. TOLUENE.

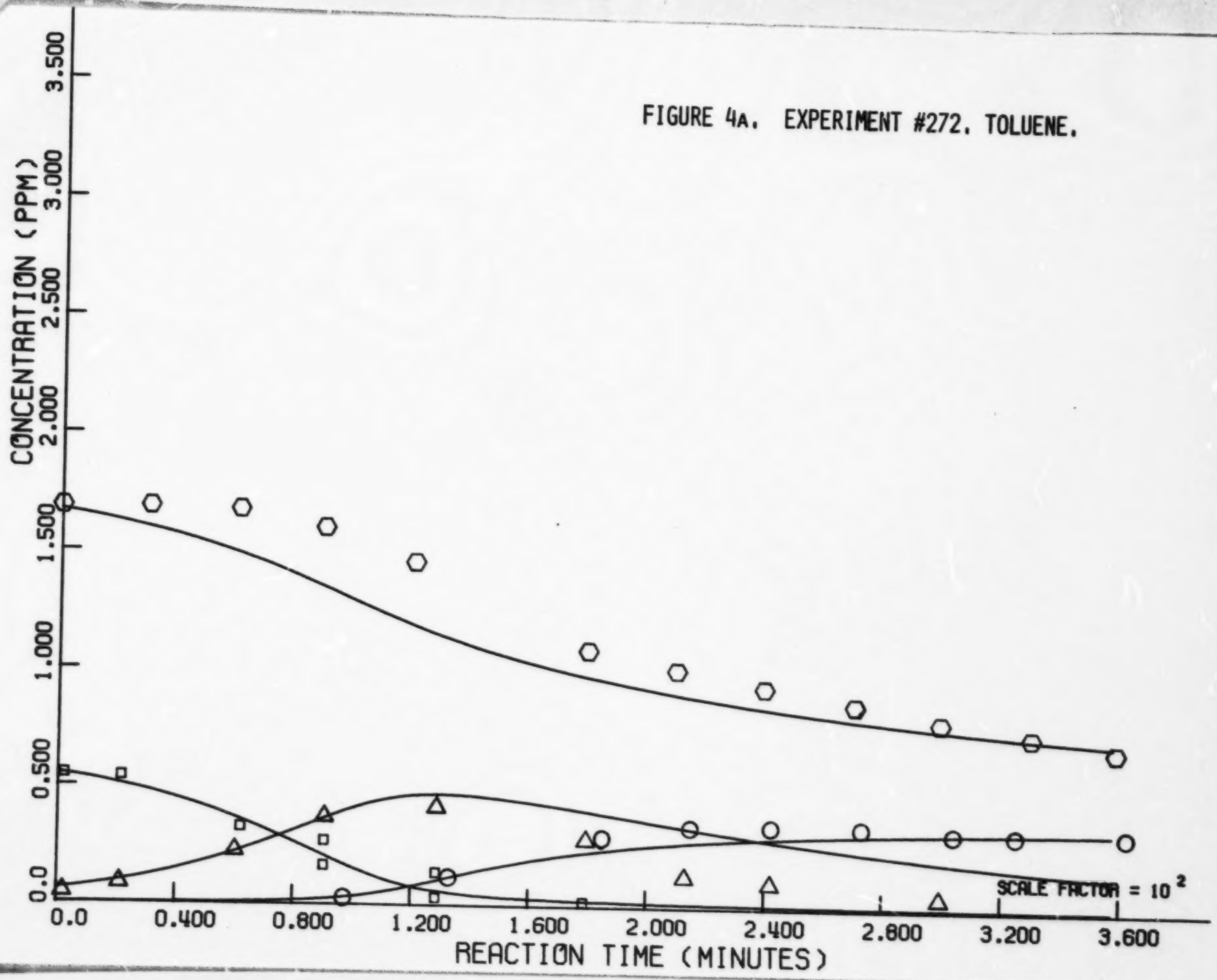

FIGURE 5. EXPERIMENT #271. TOLUENE.

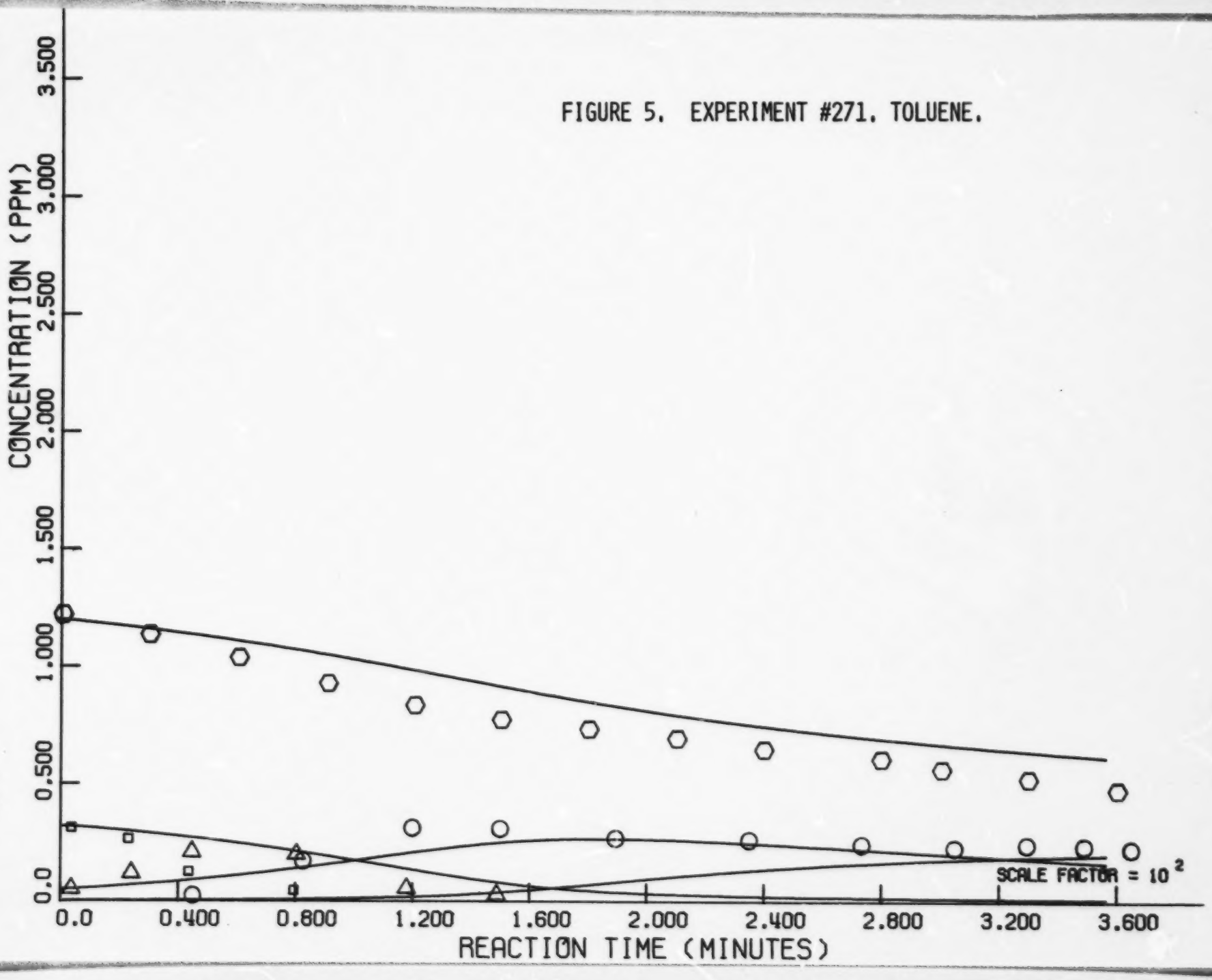

FIGURE 5A. EXPERIMENT # 271. TOLUENE.

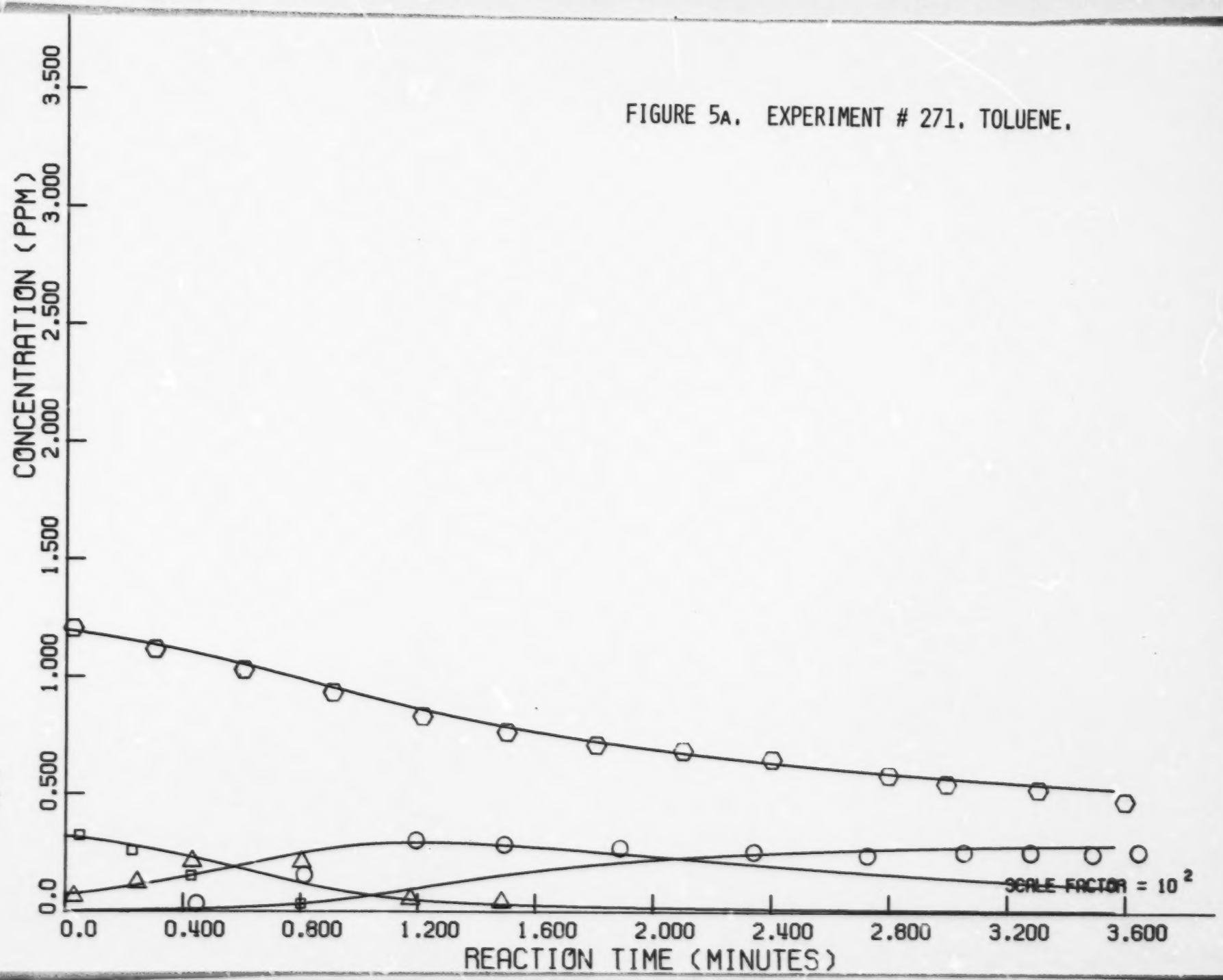

rate constant has been used, and, as before, we have assigned a small residual value for the ozone-n-butane reaction. Because n-butane should not fragment as greatly as toluene when under attack by O atoms, we have adopted a slightly smaller value of α for the former reaction ($\alpha = 5$) than for the latter. Equal values of all other stoichiometric coefficients have been assigned for each of the two species (i.e., $\beta_{toluene} = \beta_{n\text{-}butane}$, etc.). Simulation results for this system are presented in Figures 6 to 8 and 6A to 8A.

3. Propylene-Ethane-NO_x

During our preliminary examination of the propylene-ethane-NO_x data we found that the disappearance of ethane over the course of a six hour chamber run could be accounted for as losses due to sampling and dilution alone; the loss of ethane through photochemical reactions was not significant. Consequently, we treated these data as a propylene-NO_x run, considering ethane to be inert over the course of a six-hour irradiation. Values of the rate constants and stoichiometric coefficients for this system are given in Table 10.

As before, it was necessary to use a larger value for k_{11} than that reported in the literature in order to account for the loss rate of hydrocarbon and NO during the first few minutes or irradiation. In the case of propylene we adopted a value *ten times* greater than the literature value. Literature values were used for the rate constants for the reactions of propylene with OH and O_3, reactions that account for the vast majority of propylene consumed.

When propylene undergoes attack by oxygen radicals, it splits into two organic free radicals, an acyl and an alkyl radical.

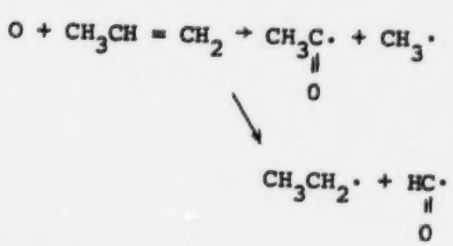

This is in contrast to the O-toluene reaction, which initially yields an alkyl radical

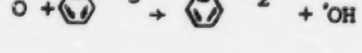

TABLE 9. Validation Parameters for Toluene-n-Butane NO_x Experiments

Rate Constants	Run 251		Run 253		Run 257	
k_1	0.266	min^{-1}	*		*	
k_2	2.76×10^6	min^{-1}	*		*	
k_3	21.8	$ppm^{-1}min^{-1}$	*		*	
k_4	0.006	$ppm^{-1}min^{-1}$	*		*	
k_5	0.1	$ppm^{-1}min^{-1}$	*		*	
k_6	5.0×10^{-4}	$ppm^{-1}min^{-1}$	*		*	
k_7	5.0×10^{-3}	min^{-1}	*		*	
k_8	-		*		*	
k_9	1.8×10^3	$ppm^{-1}min^{-1}$	*		*	
k_{10}	10.0	$ppm^{-1}min^{-1}$	*		*	
k_{11}	3.3×10^3	$ppm^{-1}min^{-1}$	3.175×10^3	$ppm^{-1}min^{-1}$	3.2×10^3	$ppm^{-1}min^{-1}$
k_{12}	9.15×10^3	$ppm^{-1}min^{-1}$	8.6×10^2	$ppm^{-1}min^{-1}$	8.7×10^3	$ppm^{-1}min^{-1}$
k_{13}	1.0×10^{-4}	$ppm^{-1}min^{-1}$	*		*	
k_{14}	1.8×10^3	$ppm^{-1}min^{-1}$	*		*	
k_{15}	16.0	$ppm^{-1}min^{-1}$	*		*	
Stoichiometric Coefficients						
α	5.35		5.29		5.30	
β	1.20		*		*	
γ	4.00		*		*	
ϵ	0.61		*		*	

* Same as for Run 251

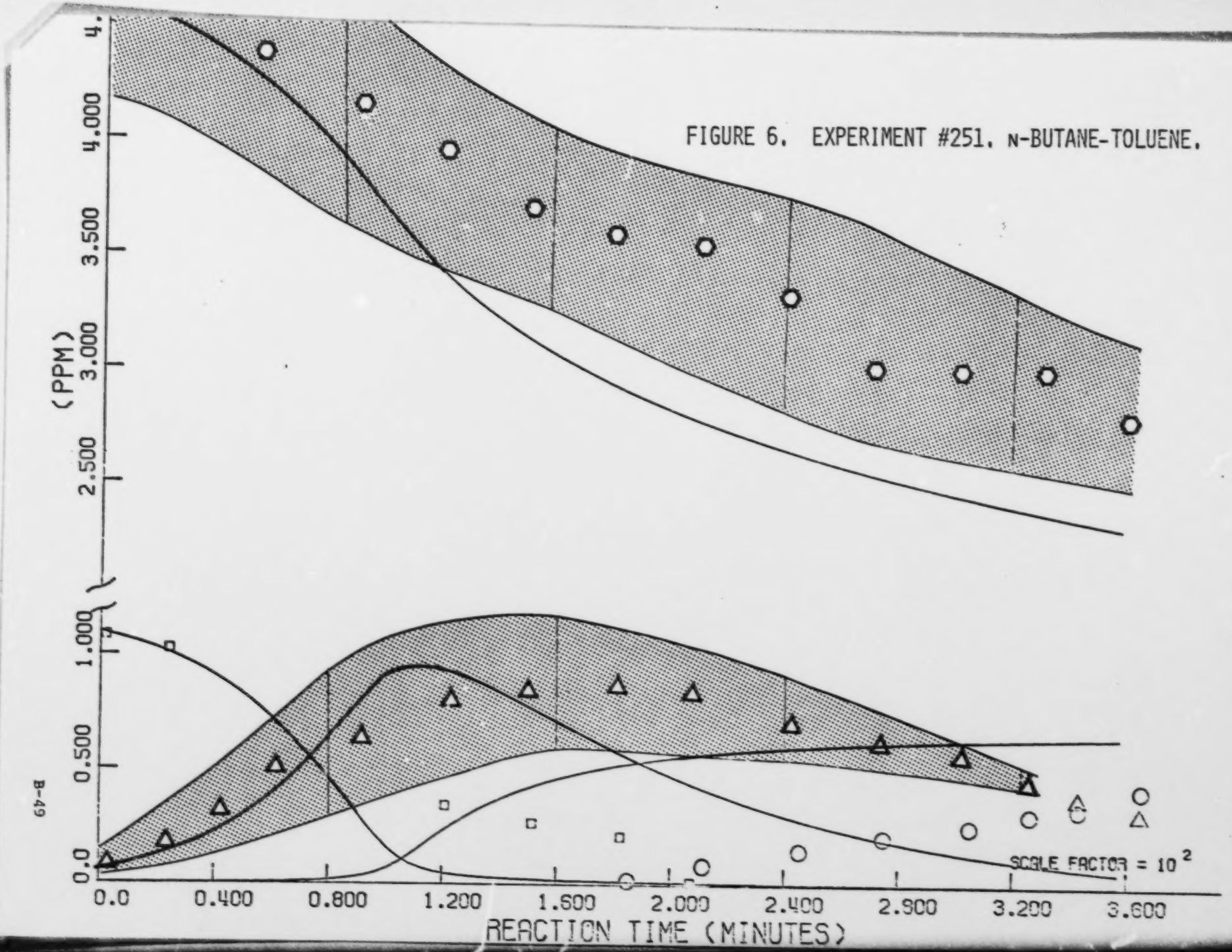

FIGURE 6. EXPERIMENT #251. N-BUTANE-TOLUENE.

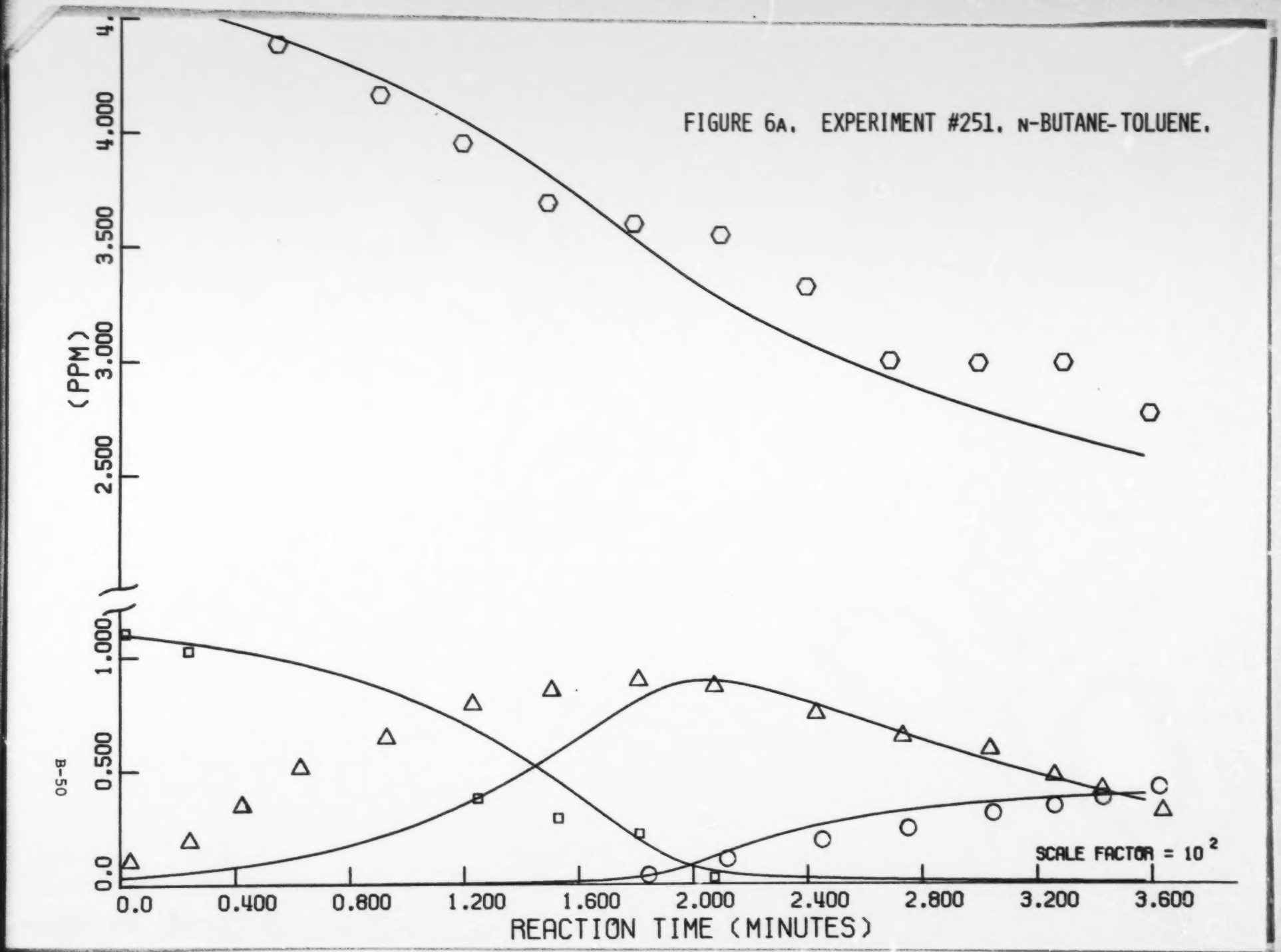
FIGURE 6A. EXPERIMENT #251. N-BUTANE-TOLUENE.
(PPM)
4.
4.000
3.500
3.000
2.500
1.000
0.500
0.0
SCALE FACTOR = 10 2
0.0
0.400
0.800
1.200
1.600
2.000
2.400
2.800
3.200
3.600
REACTION TIME (MINUTES)

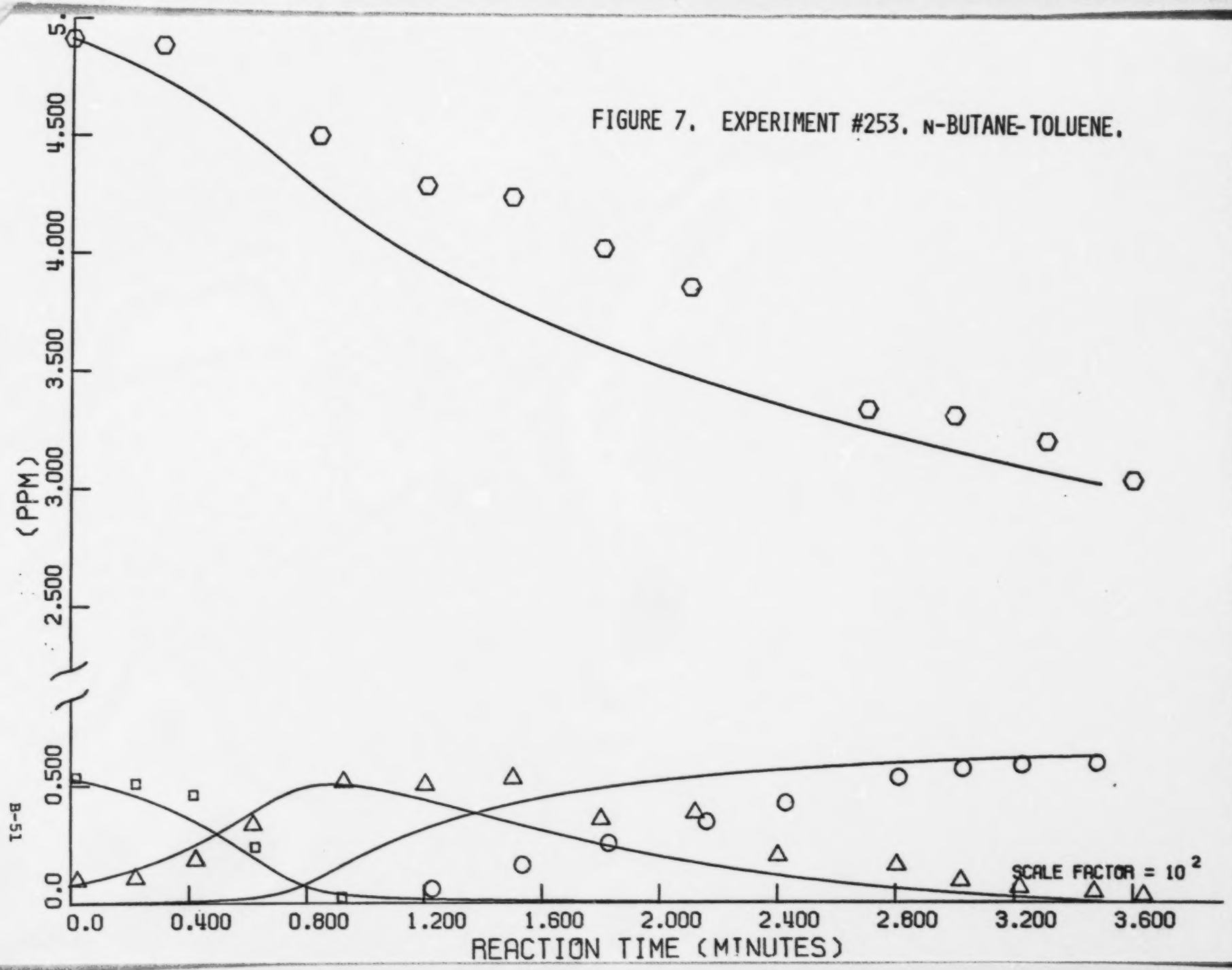

FIGURE 7. EXPERIMENT #253. N-BUTANE-TOLUENE.

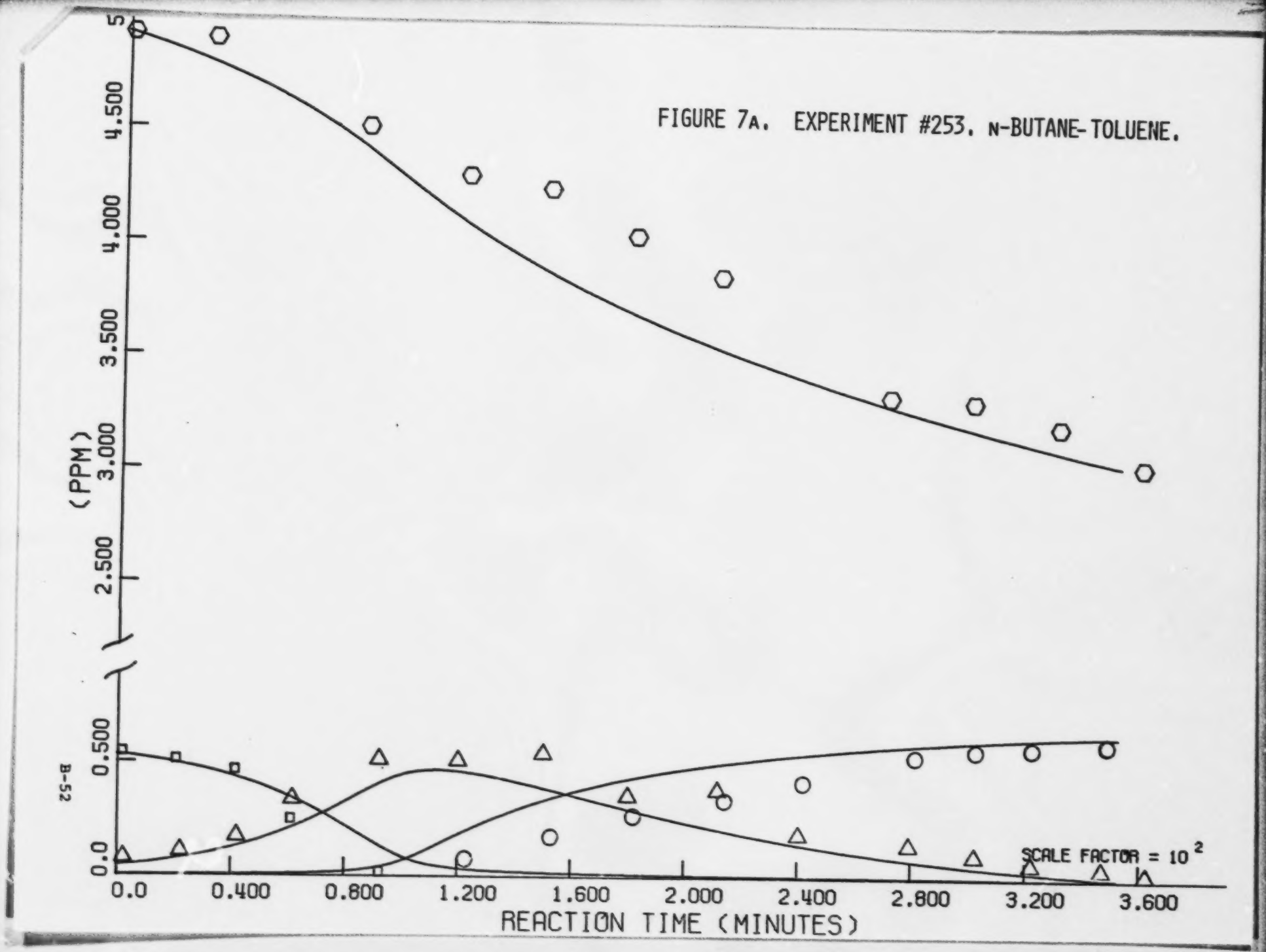
FIGURE 7A. EXPERIMENT #253. N-BUTANE-TOLUENE.
(PPM)
5
4.500
4.000
3.500
3.000
2.500
0.500
0.0
SCALE FACTOR = 10 2
0.0
0.400
0.800
1.200
1.600
2.000
2.400
2.800
3.200
3.600
REACTION TIME (MINUTES)
B-52

FIGURE 8. EXPERIMENT #257. N-BUTANE-TOLUENE

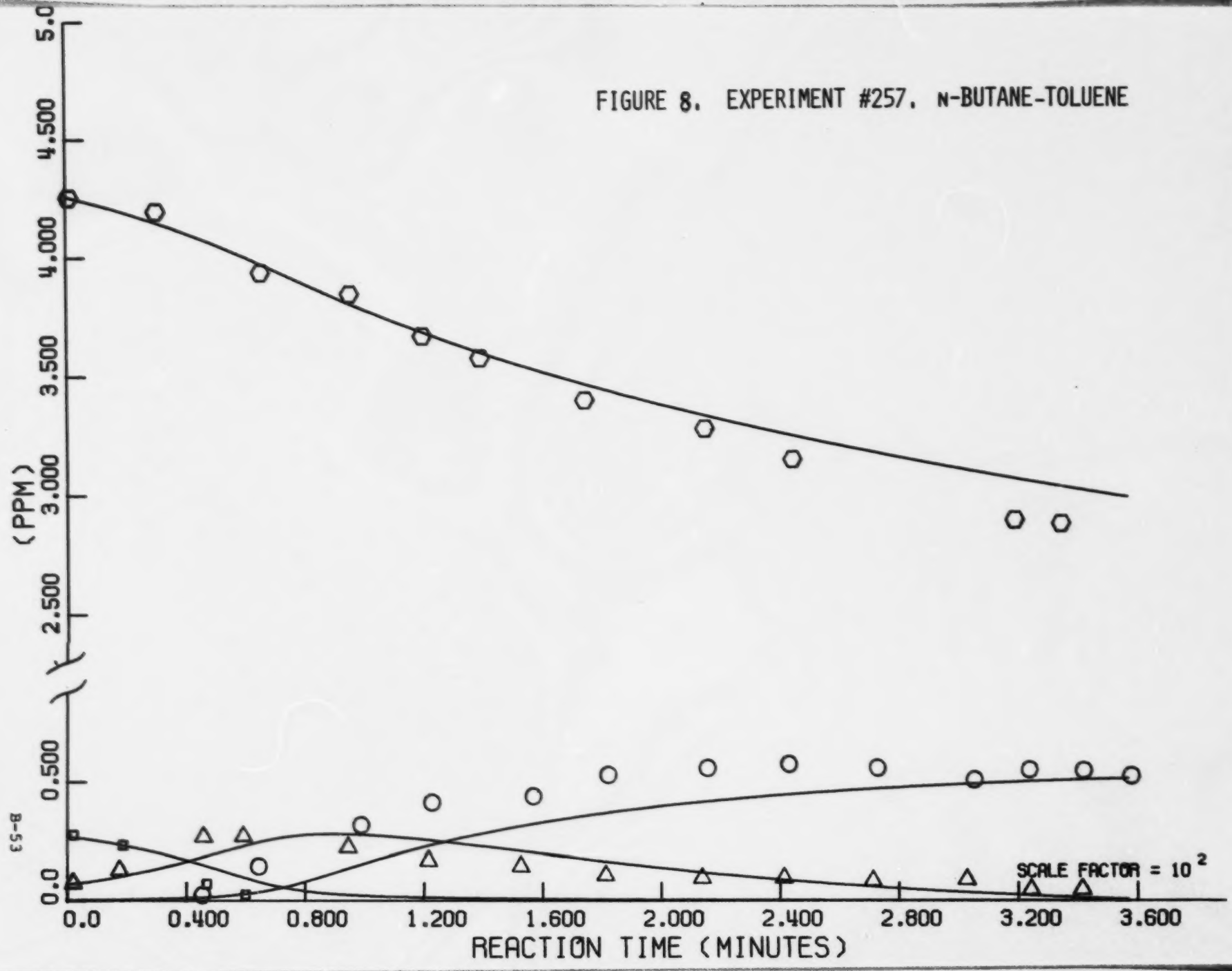

FIGURE 8A. EXPERIMENT #257. N-BUTANE-TOLUENE.

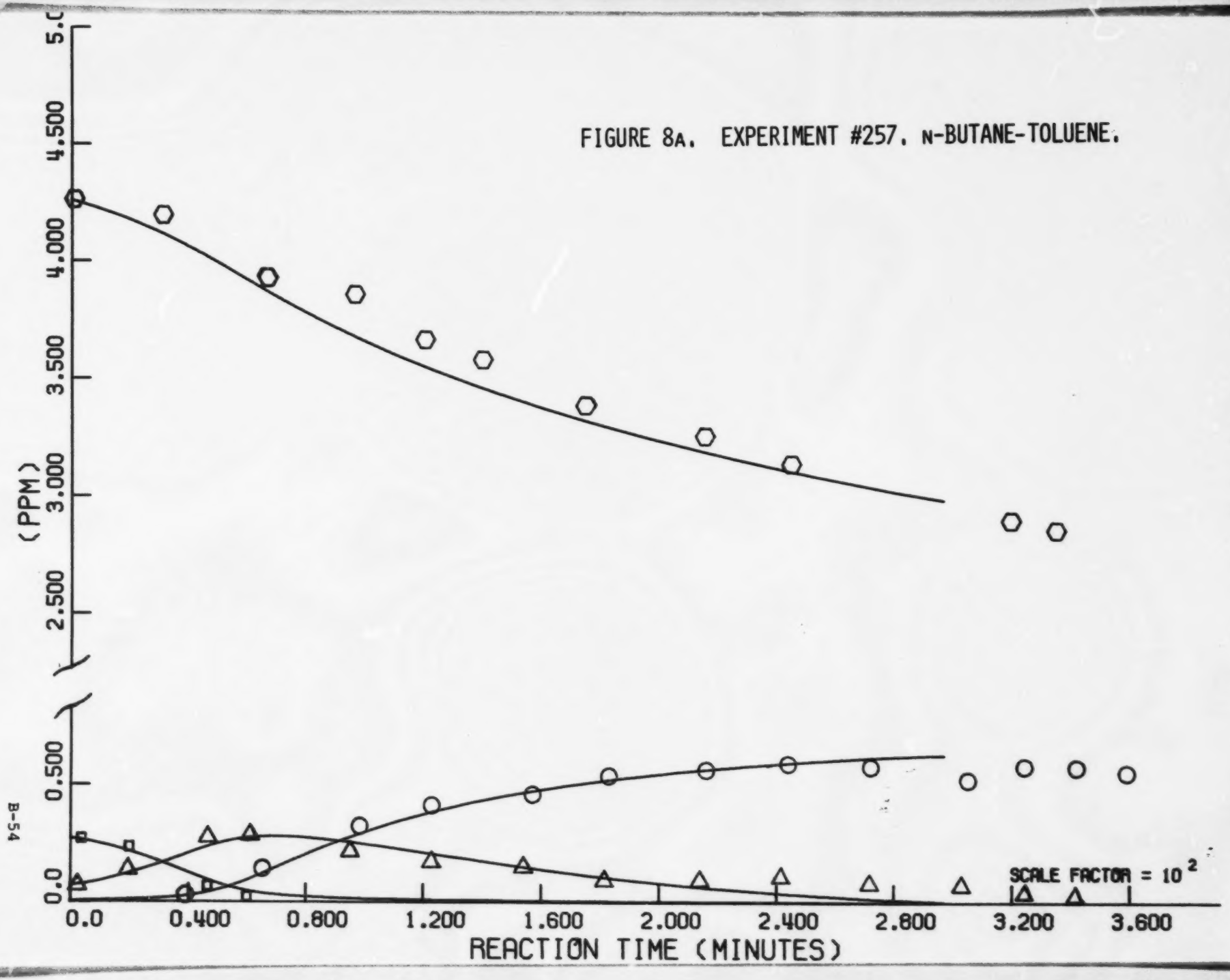

Significantly, the time to termination of a chain initiated by an acyl radical is longer than the time to termination of one initiated by an alkyl radical. This is due to the fact that the alkyl radical is a decomposition product of the acyl-initiated NO oxidation.

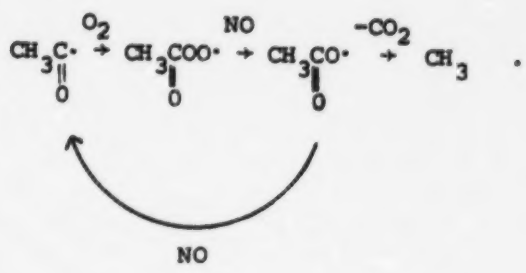

Thus, the O atom-initiated NO oxidation chain for propylene is much longer than for toluene. We have estimated that in this case, $\alpha = 16$.

As we discussed earlier, the values for β and ε are determined largely by studying the effect of CO on predicted concentrations. We established values for β and ε for isobutylene in earlier work [Seinfeld, et al. (1971)] and have used these same values for propylene. The two olefins are of similar reactivity and would thus be expected to react similarly in the presence of CO . The value of γ was established by observing the predicted oxidant formation rate and the NO_2 decay rate after the NO_2 peak. Since ozone reacts directly with propylene, the data provide a sound basis for estimation of γ . We have used this estimate of γ for all hydrocarbon systems studied thus far.

The validation results for the propylene-ethane system are presented in Figures 9-12 and 9A-12A.

4. Auto Exhaust

The auto exhaust data consist of two pairs of replicate runs obtained by irradiating auto exhaust diluted to levels approximately equal to those observed in the Los Angeles Basin.

TABLE 10. Validation Parameters for Propylene-NO_x Experiments

Rate Constants

k_1	0.266	min^{-1}
k_2	2.76×10^6	min^{-1}
k_3	21.8	$ppm^{-1}min^{-1}$
k_4	0.006	$ppm^{-1}min^{-1}$
k_5	0.1	$ppm^{-1}min^{-1}$
k_6	5.0×10^{-4}	$ppm^{-1}min^{-1}$
k_7	5.0×10^{-3}	min^{-1}
k_8	-	
k_9	1.8×10^3	$ppm^{-1}min^{-1}$
k_{10}	10.0	$ppm^{-1}min^{-1}$
k_{11}	4.0×10^4	$ppm^{-1}min^{-1}$
k_{12}	2.5×10^4	$ppm^{-1}min^{-1}$
k_{13}	0.016	$ppm^{-1}min^{-1}$
k_{14}	1.8×10^3	$ppm^{-1}min^{-1}$
k_{15}	3.0	$ppm^{-1}min^{-1}$

Stoichiometric Coefficients

α	16.0
β	0.2
γ	4.0
ε	0.22

FIGURE 9. EXPERIMENT #318. PROPYLENE.

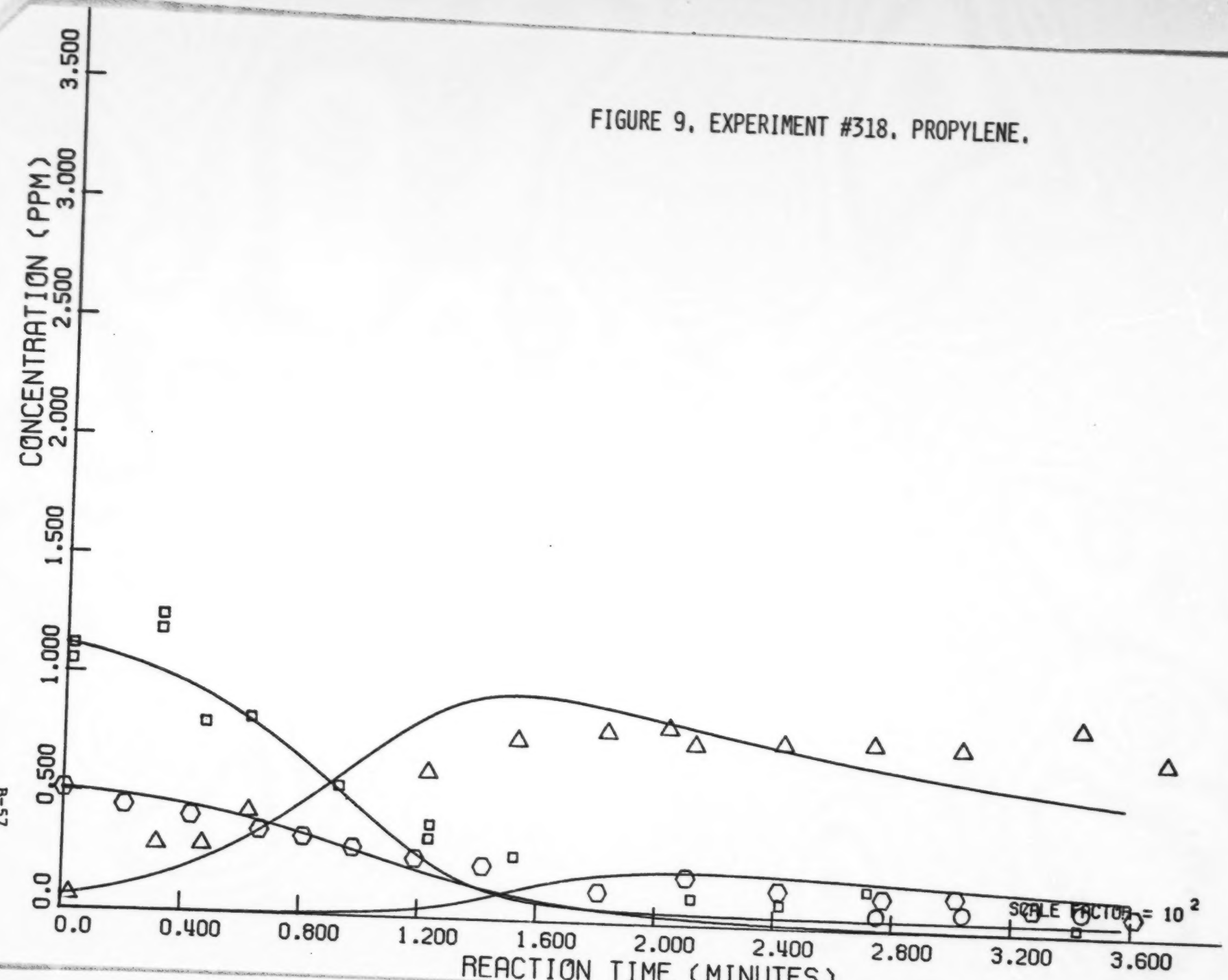

FIGURE 9A. EXPERIMENT #318. PROPYLENE.

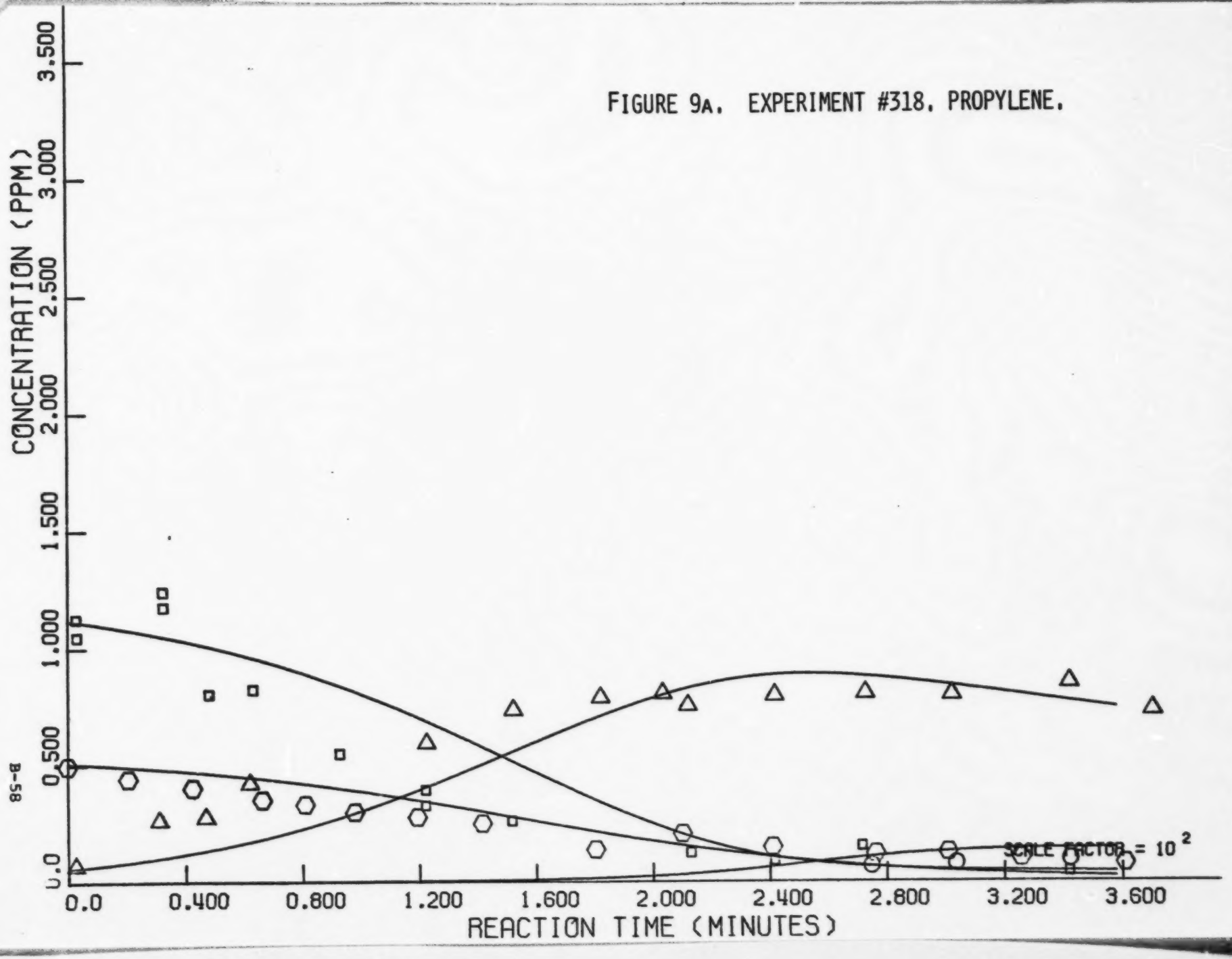

FIGURE 10. EXPERIMENT #325. PROPYLENE.

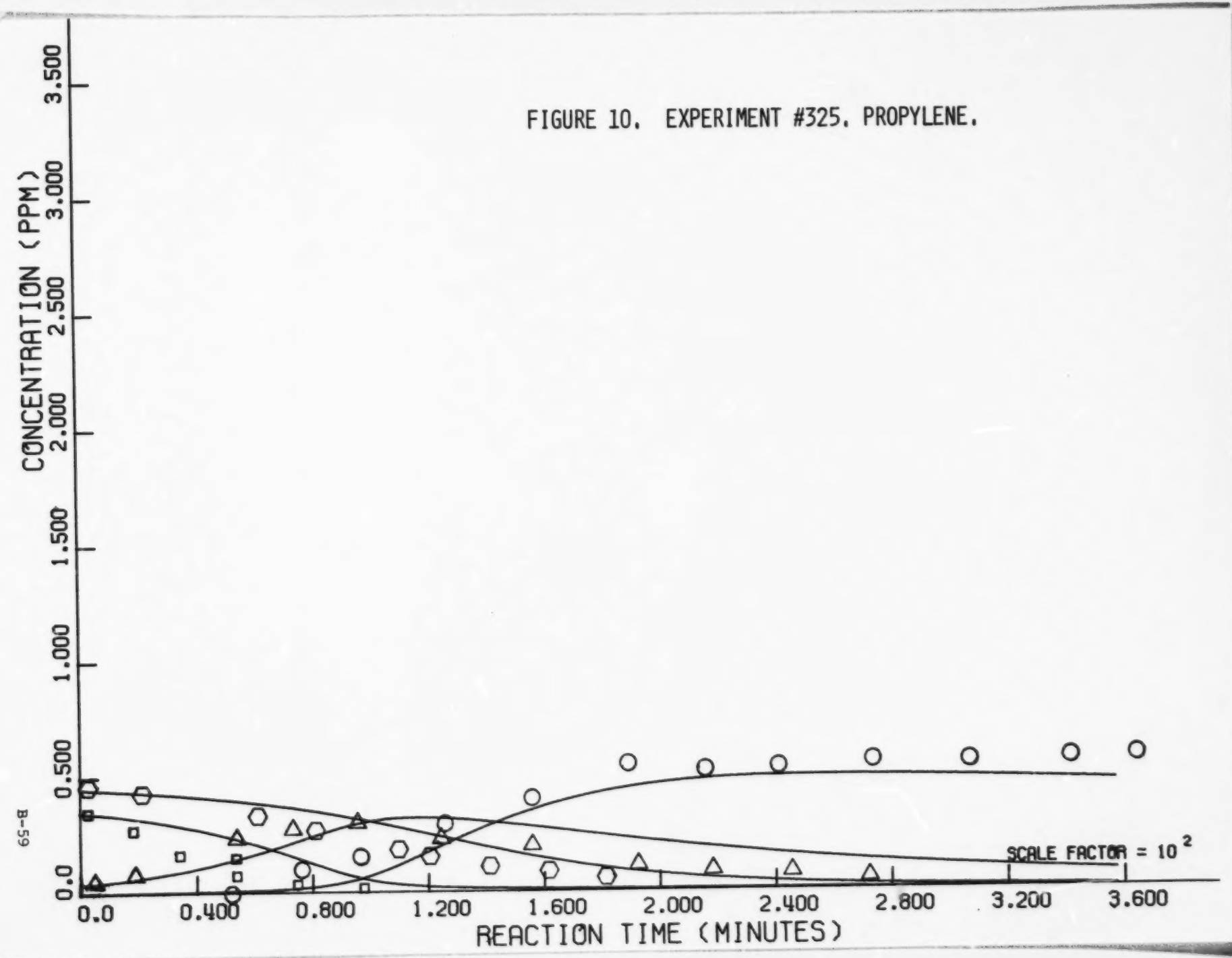

FIGURE 10A. EXPERIMENT #325. PROPYLENE.

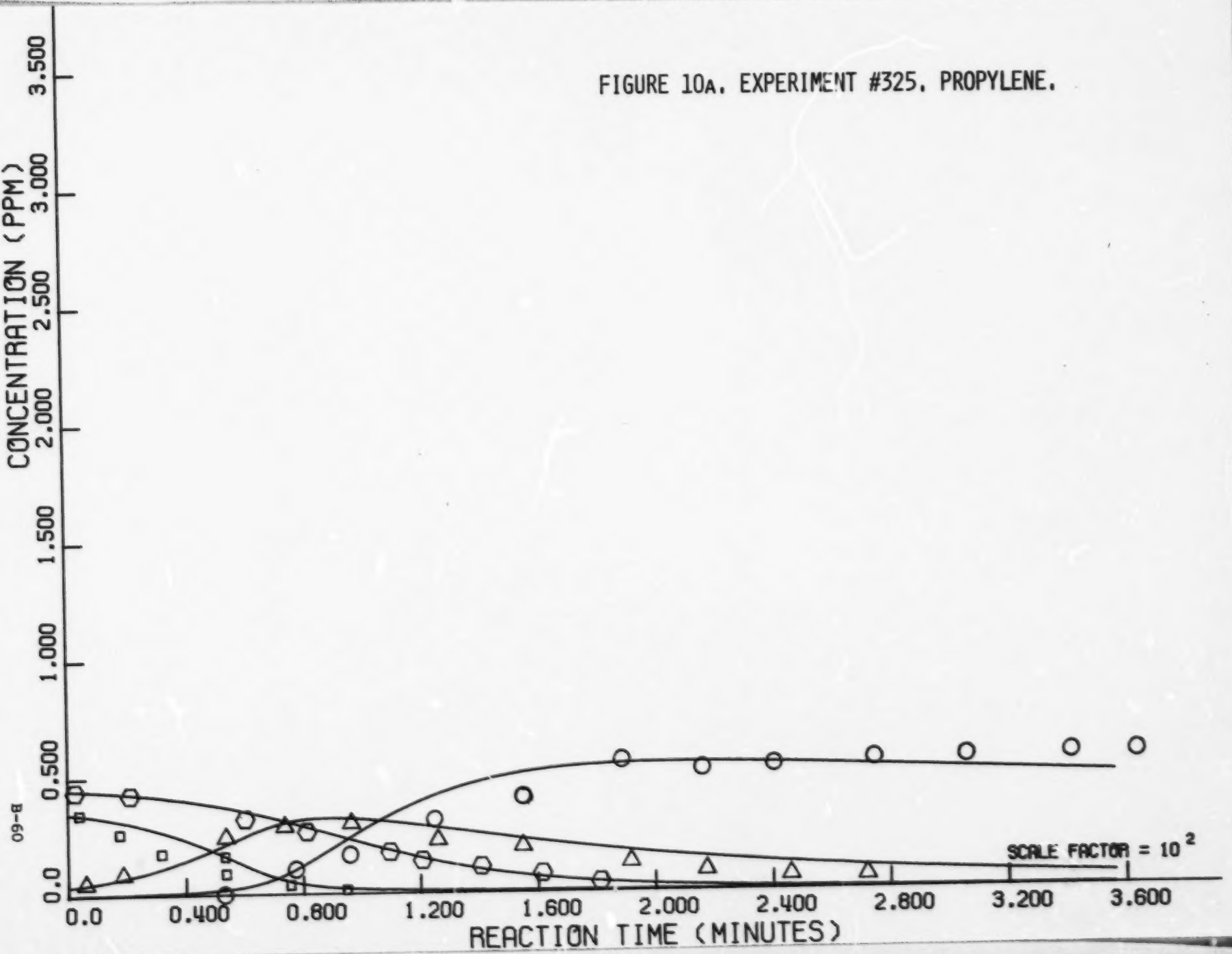

FIGURE 11. EXPERIMENT #321. PROPYLENE.

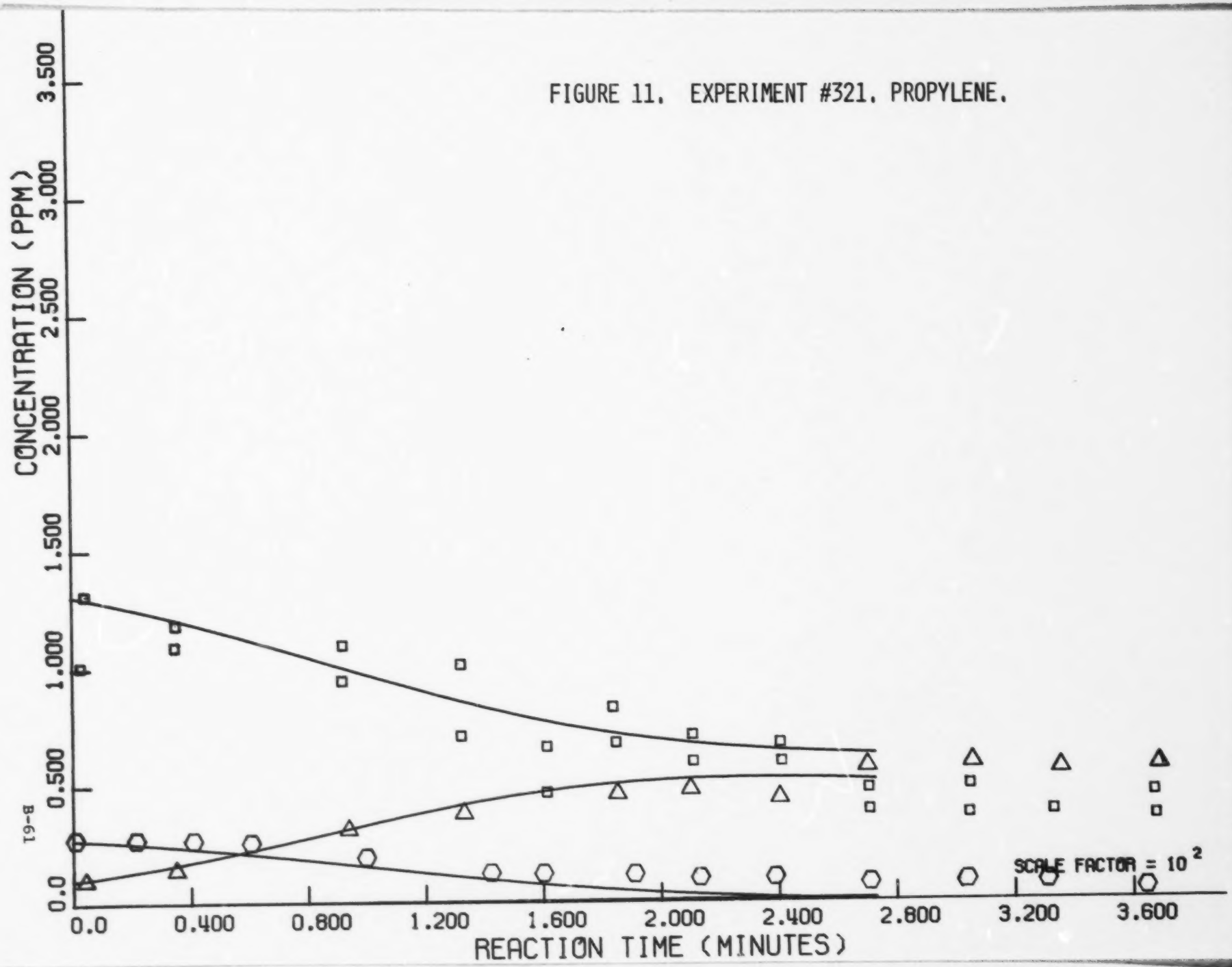

FIGURE 11A. EXPERIMENT #321. PROPYLENE.

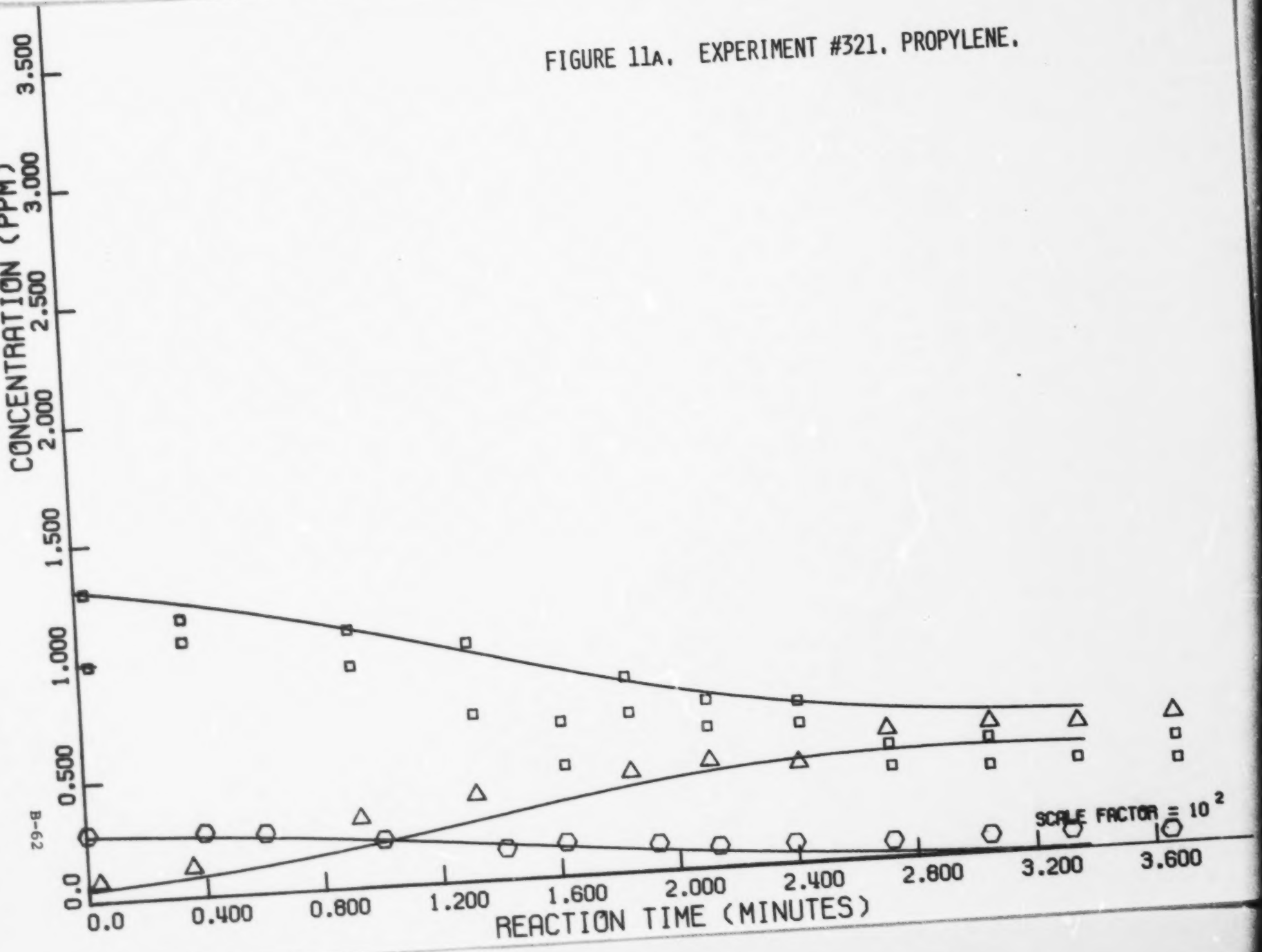

FIGURE 12. EXPERIMENT #329. PROPYLENE.

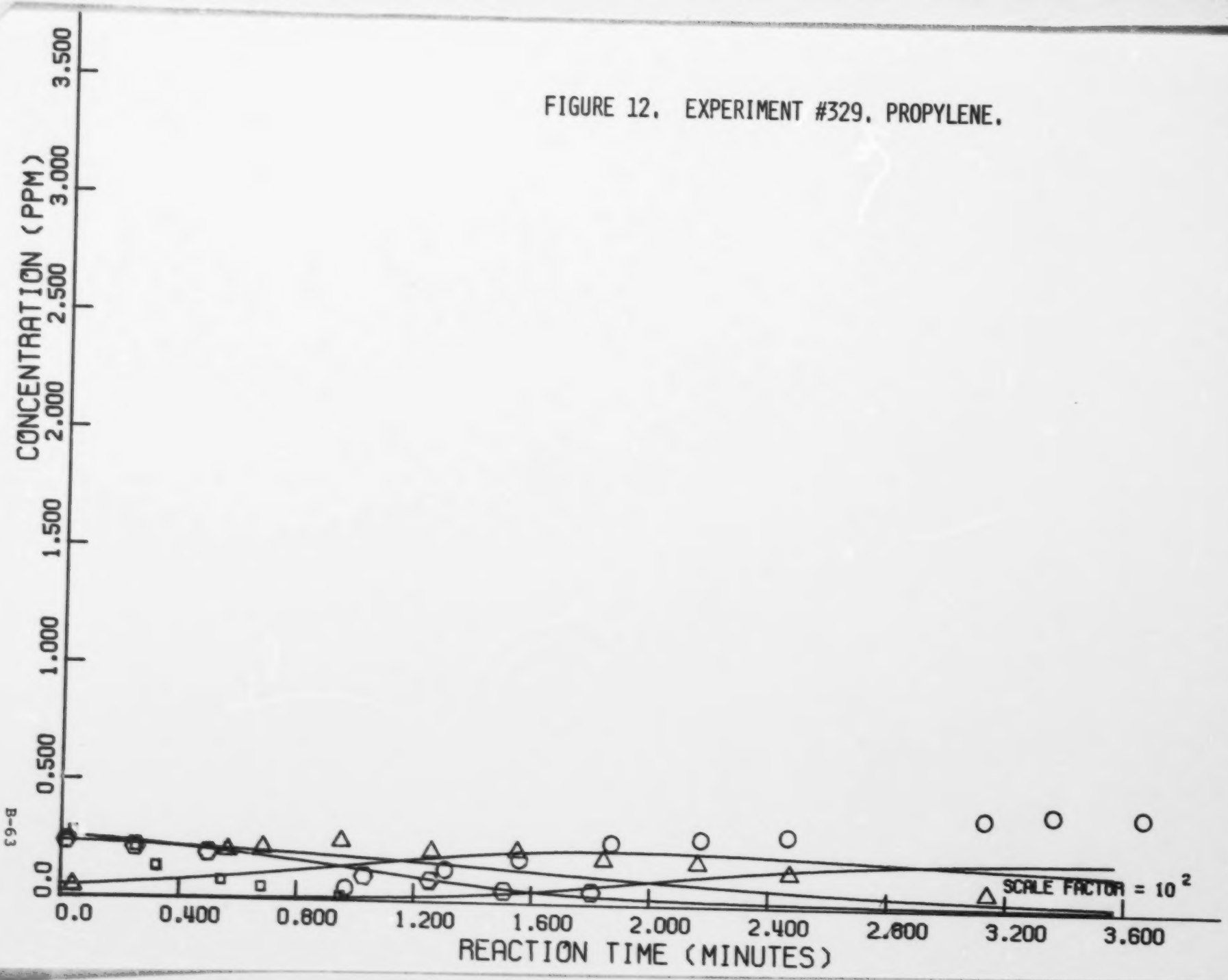

FIGURE 12A. EXPERIMENT #329. PROPYLENE.

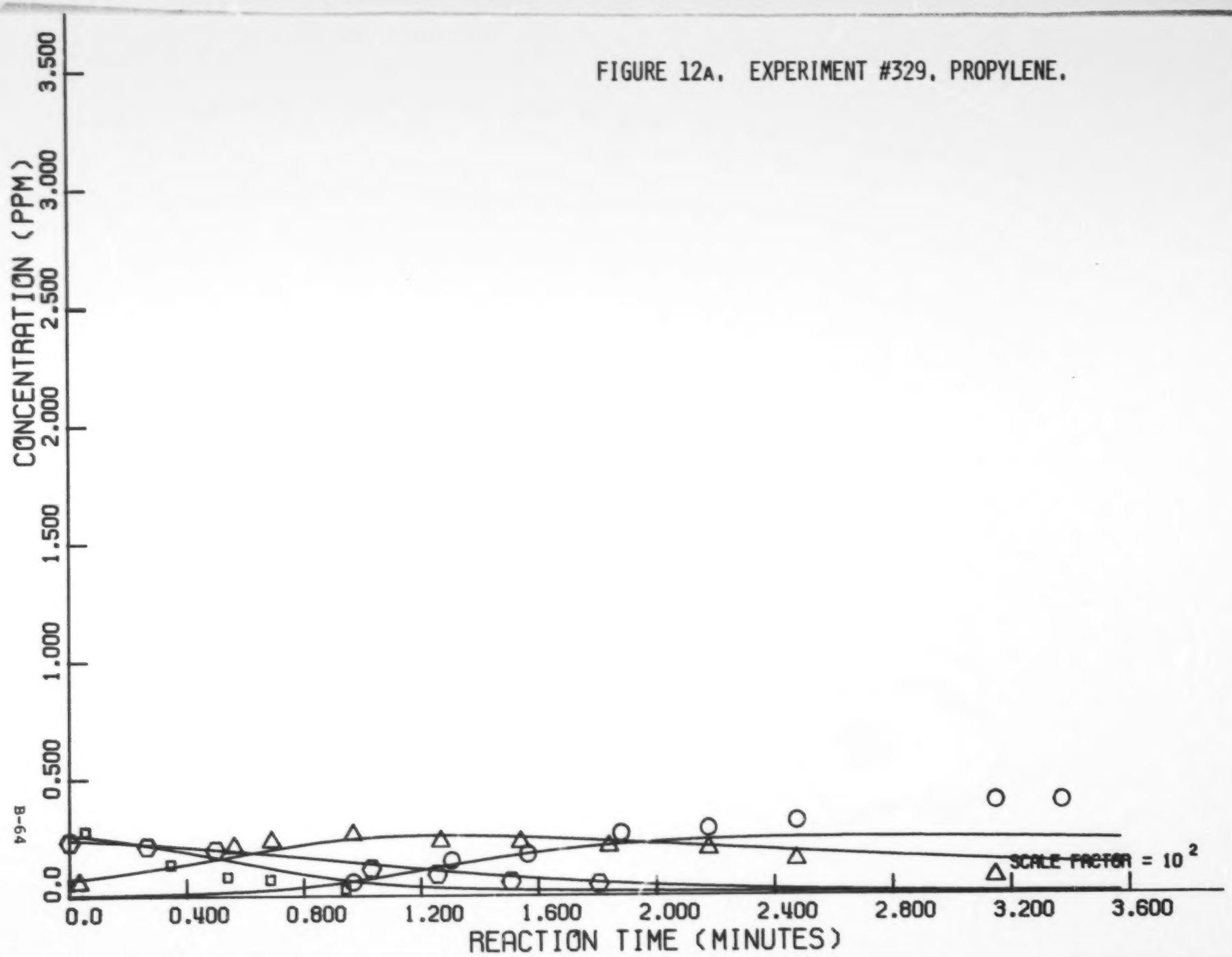

One set of data was obtained by employing as a reactant the exhaust of a Chevelle equipped with air pollution control devices. Exhaust taken from an "uncontrolled" Chevelle constituted the reactant in the second experiment. The cumulative effect of the emissions control devices was to reduce hydrocarbon and CO emissions by a factor of nearly four and to increase NO_x emissions slightly. No measurements were made of the particulate emissions from the two cars, although loss of NO_x prior to the NO_2 peak upon irradiation indicates that the particles present significantly influenced the chemical dynamics.

The hydrocarbons in the auto exhaust were analyzed in detail prior to dilution using gas chromatography. After injection into the chamber and subsequent dilution, but prior to irradiation, the hydrocarbons were analyzed again. The results of these two determinations were in poor agreement. The discrepancies observed are probably attributable to the fact that the diluted hydrocarbon species in the chamber were present at concentrations lower than those that can be accurately measured. Although it is still possible to estimate the initial hydrocarbon concentrations for these runs from the analyses made prior to dilution, hydrocarbon analyses carried out for samples collected during a chamber run are of questionable value. The hydrocarbon decay profiles shown on the validation figures have been estimated by Dr. Marcia Dodge of the Division of Chemistry and Physics. Analyses for NO , NO_2 , and oxidant were performed in the manner described earlier.

One notable difference between the irradiation results for the auto exhaust gases and those for the "pure" systems such as toluene-NO_x was that in the exhaust runs a substantial amount of NO_x was lost before the NO_2 peak. Because exhaust contains a large amount of particulate matter it has been suggested that nitrate formation might occur on particle surfaces. This is consistent with the results of Lee,et al. (1971) , who found that the nitrate content of particulate matter in exhaust that had been irradiated through the region of sharp decrease in NO and increase in NO_2 was 175 times that of the particulate matter in unirradiated exhaust. Other chamber studies of synthetic auto exhaust [Wilson, (1972)] have shown that the loss of

NO_x prior to the NO_2 peak is not observed in the absence of particulate matter. Consequently, we have included in the mechanism the additional reaction

$$NO_2 + \text{PARTICLE} \xrightarrow{19} \text{NITRATE}$$

While the exact chemical details of early NO_x loss are not yet known, inclusion of this type of reaction aids in accounting for the effect observed.

For the purpose of validating the exhaust data we elected to segment the hydrocarbons into two reactivity classes. C_4^+ paraffins and aromatics, excluding benzene, comprise the first reactivity class, ethylene and other olefins, the second reactivity class. C_1 to C_3 paraffins, benzene, and acetylene were considered to be unreactive. We further assumed that the reactivities of C_4^+ paraffins are equal to that of n-butane, that the reactivities of aromatics are equal to that of toluene, that ethylene is best treated individually*, and that the reactivities of all other olefins are equal to that of propylene. Although these assumptions obviously are subject to some question, they allow us to base our estimates of group reactivity on values established in validation runs performed previously. Moreover, the uncertainties in the hydrocarbon data do not justify a further refinement in the rate constants and stoichiometric coefficients at this time.

In order to carry out validation runs using the data described, it was first necessary to calculate the rate constant for PAN formation and the rate constants and stoichiometric coefficients for the reactions of O , OH , and O_3 with each class of hydrocarbons. As in the case of toluene-n-butane, the lumped rate constants and stoichiometric coefficients were calculated as the weighted average

* The O-ethylene rate constant was taken to be ten times the literature value, whereas all the stoichiometric coefficients were assumed to be the same as those established for propylene.

of the parameter values estimated for a pure system, weighted in proportion for the composition of the mixture. All of the lumped rate constants were calculated using the equations

$$\bar{k}_j = \frac{\sum_i k_{ij} c_i}{\sum_i c_i}$$

where k_{ij} refers to the reaction rate constant for hydrocarbon species i (for example, isobutane) and reaction j (for example, HC + O). The stoichiometric coefficients, ε and α, were calculated using the equations

$$\varepsilon = \frac{\sum_i \varepsilon_i c_i}{\sum_i c_i}$$

$$\overline{\alpha k_{11}} = \frac{\sum_i \alpha_i k_{11_i} c_i}{\sum_i c_i}$$

$$\bar{\alpha} = \frac{\overline{\alpha k_{11}}}{\overline{k_{11}}}$$

The remaining stoichiometric coefficients are not a function of the hydrocarbon composition of the reaction mixture. The base values of the rate constants and stoichiometric coefficients may be found in Table 11.

TABLE 11. Values of Base Parameters Used to Calculate Rate Constants and Stoichiometric Coefficients for Complex Hydrocarbon Mixtures*

	k_0	k_{OH}	k_{O_3}	k_{PAN}	α	β	γ	ε
C_4^+ PARAFFINS	1920	5720	.0001125	9	5	1.2	4	.61
AROMATICS (excluding benzene)	6420	15000	.000075	30	6	1.2	4	.61
ETHYLENE	7720	2500	.00287	3	16	.2	4	.22
OTHER OLEFINS	40000	25000	.0165	3	16	.2	4	.22

* Reaction rate constants are given in $ppm^{-1}min^{-1}$

Estimates of the rate constants for the lumped hydrocarbon and PAN formation reactions were based on initial compositions of the reactant mixture. However, samples were drawn from the chamber during the course of the experiment and were analyzed chromatographically to determine their hydrocarbon composition. As a result, we were able to calculate updated estimates of the high reactivity hydrocarbon reaction rate constants at two times--

- the time at which half of the initial NO had disappeared
- the time at which the NO_2 peak occurred.*

The effect of updating the high reactivity rate constant at the two times was to lower the reactivity of the class since ethylene, having a lower reactivity than the other olefins, increased in its percentage composition with time. The reactivity of the low reactivity hydrocarbon class appeared to remain essentially constant throughout the period of irradiation.

We assumed for the purposes of validation that the concentration of CO was constant throughout each run. Losses of CO are incurred, however, through reaction with OH radicals and as a result of sample withdrawal. Also, CO is formed when formyl radicals and other products decompose. Carbon monoxide enters into the chemical dynamics most prominently between the times when irradiation commences and when the NO_2 peak occurs. The loss of CO during this period was probably less than 10 percent.

Attempts at validating the model for exhaust obtained from the unequipped Chevelle revealed that our estimated, a priori values of the stoichiometric coefficients were too high, that is, the NO oxidized too rapidly. In order to

* Due to suspected uncertainties in the chromatographic analyses we did not attempt to continuously update the estimates of the rate constants. Also, as such a calculation depends upon having knowledge of the measured values, it is not a particularly desirable procedure.

obtain improved validation results we found it necessary to use values of α , α_2 , β , β_2 and γ that are twenty percent lower than those originally calculated. Experimentally, the slower loss of NO might have occurred because the presence of particles enhanced the rate of chain termination, thus reducing radical chain length. It is also possible that the CO is not treated properly in the model. Finally, we assumed that the value of k_1 was at the lower end of the uncertainty range, or 0.166 $min.^{-1}$.

In carrying out validation runs for exhaust collected from the equipped Chevelle, we used the mean light intensity and the a priori values of the stoichiometric coefficients. Reasonably good predictions were obtained for the NO loss and NO_2 production rates, but the hydrocarbon disappeared much too rapidly. A twenty percent reduction in the radical chain lengths and a lower light intensity would have resulted in a better hydrocarbon validation but much poorer results for the NO_x . Because the hydrocarbon data are of doubtful accuracy, especially in this run, we chose not to make the 20% reduction. Also, it is not possible to assess the accuracy of assuming shorter radical chain lengths or loss of NO_2 to particles, as no characterization of the particles was attempted experimentally (i.e., the number and size distribution of the particles, the chemical composition of the particles, and the magnitude of light scattering due to the particles). Making the assumptions cited, however, constitutes one means of obtaining improved validations and, as a result, perhaps merits further investigation experimentally.

The rate constants used for auto exhaust simulation runs are listed in Tables 12 and 13, and the validation results are presented in Figures 13 and 14.

TABLE 12. Validation Parameters for Auto Exhaust Experiments (Unequipped Chevelle)

Rate Constants	Run 222	
k_1	0.166	min^{-1}
k_2	2.76×10^{6}	min^{-1}
k_3	21.8	$ppm^{-1}min^{-1}$
k_4	0.006	$ppm^{-1}min^{-1}$
k_5	0.1	$ppm^{-1}min^{-1}$
k_6	5×10^{-4}	$ppm^{-1}min^{-1}$
k_7	5×10^{-3}	min^{-1}
k_8	1.06×10^{4}	min^{-1}
k_9	1.8×10^{3}	$ppm^{-1}min^{-1}$
k_{10}	10.0	$ppm^{-1}min^{-1}$
k_{11}	3.83×10^{3}	$ppm^{-1}min^{-1}$
k_{12}	9.51×10^{3}	$ppm^{-1}min^{-1}$
k_{13}	9.8×10^{-5}	$ppm^{-1}min^{-1}$
k_{14}	1.8×10^{3}	$ppm^{-1}min^{-1}$
k_{15}	10.6	$ppm^{-1}min^{-1}$
k_{16}	2.54×10^{4}	$ppm^{-1}min^{-1}$
k_{17}	1.48×10^{4}	$ppm^{-1}min^{-1}$
k_{18}	0.01	$ppm^{-1}min^{-1}$
k_{19}	5×10^{-3}	min^{-1}

Stoichiometric Coefficients	
α	4.56
β	0.96
γ	3.20
ϵ	0.415
α_2	12.8
β_2	0.16
γ_2	3.2

At a time half way to the NO_2 peak, the following changes were made:

k_{16}	2.5×10^{4}	$ppm^{-1}min^{-1}$
k_{17}	1.45×10^{4}	$ppm^{-1}min^{-1}$

At the time of the NO_2 peak, the following changes were made:

k_{16}	2.12×10^{4}	$ppm^{-1}min^{-1}$
k_{17}	1.19×10^{4}	$ppm^{-1}min^{-1}$
k_{18}	8.5×10^{-3}	$ppm^{-1}min^{-1}$

TABLE 13. Validation Parameters for Auto Exhaust Experiments (Equipped Chevelle)

Rate Constants	Run 231	
k_1	0.266	min^{-1}
k_2	2.76×10^{6}	min^{-1}
k_3	21.8	$ppm^{-1}min^{-1}$
k_4	0.006	$ppm^{-1}min^{-1}$
k_5	0.1	$ppm^{-1}min^{-1}$
k_6	5.0×10^{-4}	$ppm^{-1}min^{-1}$
k_7	5.0×10^{-3}	min^{-1}
k_8	2.4×10^{3}	min^{-1}
k_9	1.8×10^{3}	$ppm^{-1}min^{-1}$
k_{10}	10.0	$ppm^{-1}min^{-1}$
k_{11}	3.96×10^{3}	$ppm^{-1}min^{-1}$
k_{12}	9.9×10^{3}	$ppm^{-1}min^{-1}$
k_{13}	9.6×10^{-5}	$ppm^{-1}min^{-1}$
k_{14}	1.8×10^{3}	$ppm^{-1}min^{-1}$
k_{15}	8.24	$ppm^{-1}min^{-1}$
k_{16}	2.18×10^{4}	$ppm^{-1}min^{-1}$
k_{17}	1.23×10^{4}	$ppm^{-1}min^{-1}$
k_{18}	5.0×10^{-3}	$ppm^{-1}min^{-1}$
k_{19}	5.0×10^{-3}	min^{-1}

Stoichiometric Coefficients	
α	5.73
β	1.20
γ	4.00
ε	0.352
α_2	16.0
β_2	0.2
γ_2	4.0

FIGURE 13. EXPERIMENT #222, AUTO EXHAUST

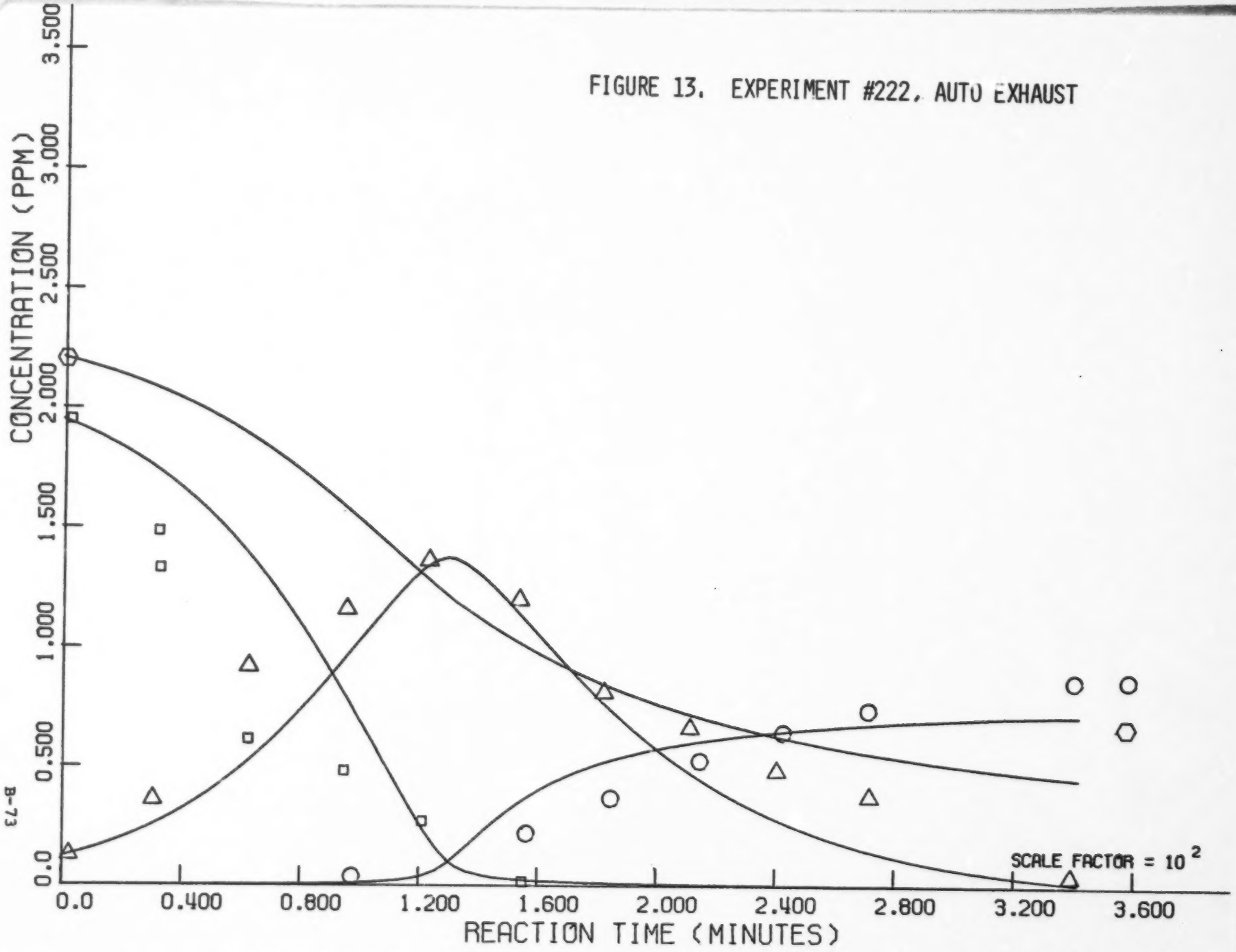

FIGURE 14. EXPERIMENT #231, AUTO EXHAUST.

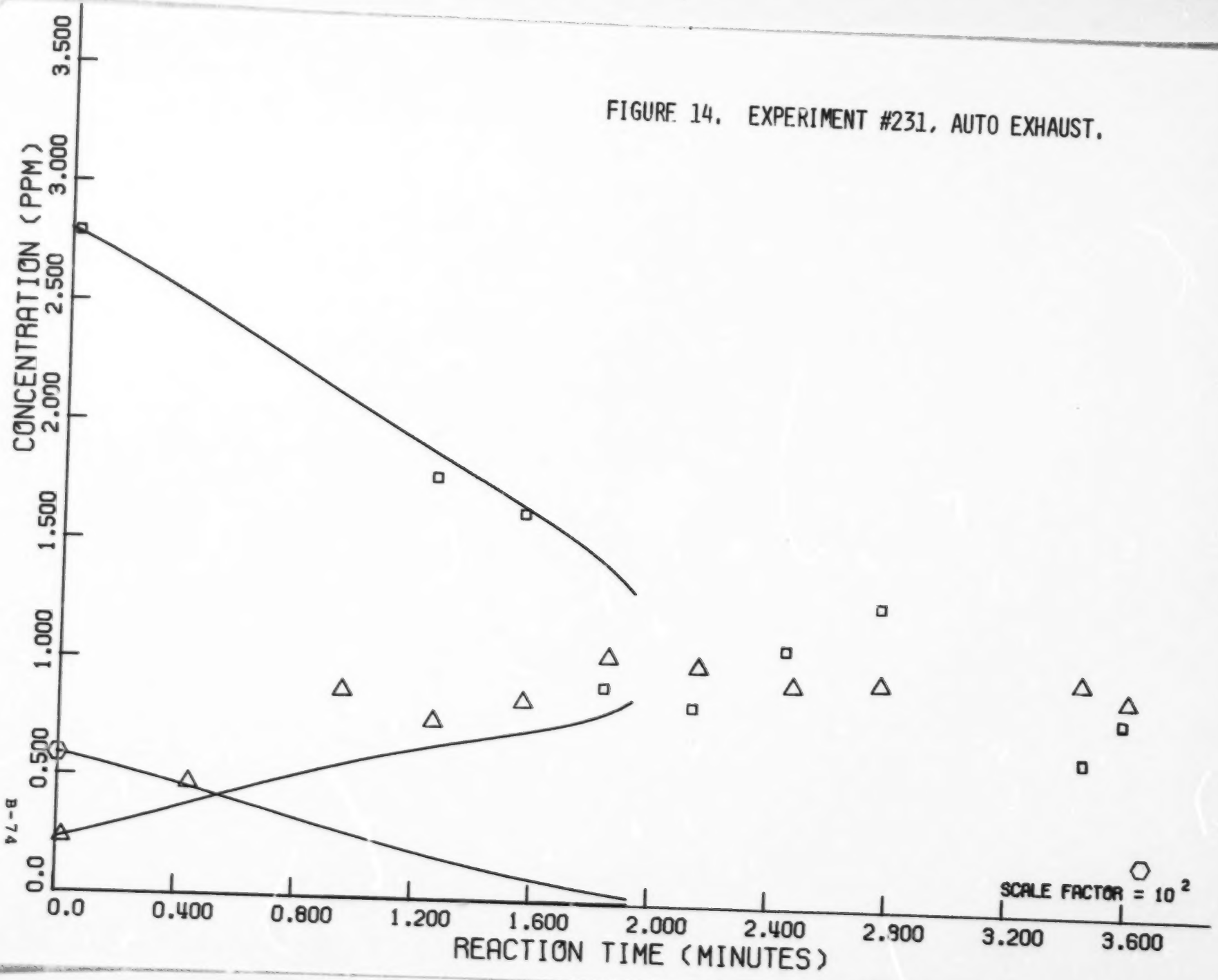

V. CONCLUDING COMMENTS

The data base provided for the validation studies fulfills many of the important requirements that one would wish to place on it. The concentration levels of the hydrocarbons, nitrogen oxides, and oxidants are representative of those observed during smoggy days in Los Angeles. Initial conditions for the runs covered a broad range of hydrocarbon to nitrogen oxide ratios. This is a particularly important property of the data base if the validated mechanism is to be part of an airshed model which will be used to evaluate proposed alternative control strategies. On the whole, the accuracy and precision of the measurements is adequate, although there are a number of important exceptions, which we will mention shortly.

An important aspect of the data base is the variety of hydrocarbon systems included. High, intermediate and low reactivity hydrocarbons were represented, as were single reactants (toluene and propylene) and a binary mixture. Moreover, a complex and highly realistic mixture, auto exhaust, is included, serving as an important test of the model. A useful addition to the four reactant systems studied would be a binary mixture of high and intermediate or low reactivity hydrocarbons, perhaps propylene and toluene.

While the data base possesses many desirable attributes, its shortcomings must be noted as well, for these determine the limits within which the model may be tested. Consider, for example, a data base for which concentrations have been determined with only passable accuracy. Wide ranging sets of parameters could easily produce predictions all of which fall within the broad limits of experimental uncertainty. Under such circumstances, it is not possible to satisfactorily test the adequacy of the mechanism to represent the data.

We have mentioned the most notable deficiencies of the data base at one point or another in earlier sections. We summarize them here, with some comments.

- Inaccuracy in measurement and in analytical procedure. As noted earlier, Mast and KI readings were badly discrepant, initial NO_2 was imprecisely determined, and light intensity was not known with sufficient accuracy. Also NO and NO_2 determinations were inaccurate at low concentrations, and hydrocarbon analyses prior to and subsequent to injection into the chamber were in poor agreement. We recommend the use of chemiluminescent techniques for NO_x and O_3 analyses in future studies, the careful determination of k_1 by an accurate technique [see, for example, Holmes, et al. (1972)], and determination of the cause of discrepancies in hydrocarbon analyses.

- Lack of measurement of certain species, both in the gas phase and on the wall. It would be of value to monitor nitric and nitrous acid concentrations in future studies. Determination of wall concentrations of these species is also desirable.

- Lack of control of water concentration.

- Lack of controlled variation of CO concentration. CO was present only in the auto exhaust runs; its influence on rate processes is best determined by allowing it to vary over a broad range in concentrations in simple hydrocarbon systems.

- Complete lack of characterization of particles in the auto exhaust experiments. Information concerning size, number and chemical composition is needed. Also, we would wish to determine the degree to which size and number distribution of the exhaust are altered due to deposition and absorption on the sampling container, and, after injection into the chamber, during the chamber sampling procedure.

Turning now to the results of the validation efforts, we make a number of observations. First, we have been able to demonstrate that, in general, there is acceptable agreement between predicted and measured concentrations. In making this statement, we must emphasize that substantial uncertainties exist in the magnitude of light intensity and initial NO_2 concentration, as well as in the values of measured concentrations of HC , NO , NO_2 and O_3 , thus limiting the possibilities for critically testing the adequacy of the model. More specifically, the mechanism has shown good qualitative and quantitative agreement with observed values of the time to the NO_2 peak and final ozone levels reached for a wide range of hydrocarbon to NO_x ratios. This agreement was achieved using fixed values of rate constants and stoichiometric coefficients (except where these constants are known to vary with composition) for all validation runs for a given reactant system.

Prior to undertaking the validation runs we carried out a limited and informal sensitivity study. The results of the study indicated that k_1 and $NO_2|_o$ had a large effect on predicted concentrations. As the uncertainty in the magnitude of these parameters was considerable

$$k_1 = 0.266 \pm .10 \text{ min.}^{-1}$$

$$NO_2|_o = \text{measured value} \pm 50\% \quad ,$$

we elected to carry out simulation runs using both (1) base parameter values and (2) base parameter values, with k_1 and/or $NO_2|_o$ varied within their uncertainty limits in such a way as to improve the predicted concentration/time profiles. In general, discrepancies between predicted and observed concentrations were reduced considerably when "improved" values of k_1 and $NO_2|_o$ were used. The sensitivity of the model to these parameters highlights the need for more accurate and precise determination of key experimental variables and parameters if the adequacy of the mechanism is to be critically evaluated.

The grouping or "lumping" of hydrocarbons in complex reactant systems is a topic which will require further study. How many groupings are needed? How shall they be segmented? How shall we estimate the "lumped" rate constants and stoichiometric coefficients? As the number of hydrocarbon groupings in the model, and thus the level of detail and complexity, increases, so does the opportunity for more accurate representation. But with the increase in complexity there is an increase in computation and storage requirements and in the amount and quality of data needed. In this study we have chosen to divide the hydrocarbons into three classes:

(1) high reactivity hydrocarbons consisting of olefins

(2) low reactivity hydrocarbons consisting of C_4^+ paraffins and all aromatics except for benzene

(3) non-reactive hydrocarbons consisting of C_1 to C_3 paraffins, benzene and acetylene.

For extremely complex systems, such as actual atmospheric mixtures, usually relatively little is known concerning the hydrocarbon composition and its variation in space and time. Moreover, emissions rates and composition, and their spatial and temporal variations, are usually poorly determined. In such cases there would be little advantage in dividing the hydrocarbons in this manner. Rather, one might lump all reactive hydrocarbons into a single reactivity class, leaving only those species that are essentially unreactive to be included in a second grouping.

Once the three groupings of hydrocarbons were selected it was necessary to establish values of "lumped" parameters. We assumed throughout that the "lumped" rate constants and stoichiometric coefficients could be estimated quite simply as weighted averages of the individual parameters, the weights being equal to the fraction of each species present in the hydrocarbon mixture. The validation results suggest that this procedure is quite satisfactory, given the limitations in accuracy of the data. However, future validation studies, involving more precise data, will provide a better test of this assumption.

To conclude, we believe that the validation results reported here indicate that the mechanism provides an adequate, perhaps good, description of smog chamber kinetics. In particular, the model appears capable of predicting the concentration/time behavior of a variety of reactant systems over a wide range of initial conditions. The few auto exhaust simulations performed indicate that the mechanism displays promise for describing the complex mixtures that exist in the atmosphere. The guidelines established for estimating rate constants and stoichiometric coefficients also have proven to be quite adequate. However, a considerably more accurate and complete data base is required if the adequacy of the model is to be critically evaluated. We recommend that a carefully conceived experimental program be undertaken for the sole purpose of providing the data needed to carry out such an evaluation.

With regard to the status of the present model, it would perhaps be useful to carry out further validation studies using existing data, if these data fill a gap in the data base that has been employed thus far. For example, it would be valuable to perform simulations for a mixture of high and low reactivity hydrocarbons. It may also be useful to carry out validations for reactant systems similar to those studied by us, but where the experiments were performed in smog chambers having different configurations, sizes, wall materials, etc. However, we do not believe that is is appropriate to undertake additional validation studies for "fine tuning" of the model; existing data cannot support such an effort. More accurate and complete data bases are required for this purpose, data bases that do not suffer from the deficiencies listed earlier in this section.

REFERENCES

Altshuller, A.P., Kopczynski, S.L., Lonneman, W.A., Becker, T.L., Slater, R., Environ. Sci. Tech., 1, 889 (1967a).

Altshuller, A.P., Kopczynski, S.L. Lonneman, W.A., Sutterfield, F.D., Wilson, D.L., Environ. Sci. Tech., 4, 44 (1970).

Altshuller, A.P., Kopczynski, S.L., Lonneman, W., Wilson, D., J. Air Pollution Control Assn., 17, 734 (1967b).

Altshuller, A.P., Kopczynski, S.L., Wilson, D., Lonneman, W., Sutterfield, F.D., J. Air Pollution Control Assn., 19, 791 (1969).

Dodge, M.C., Bufalini, J.J., "The Role of Carbon Monoxide in Polluted Atmospheres," Environmental Protection Agency, Research Triangle Park, North Carolina 27711 (1972).

Gay, B.W., Jr., Bufalini, J.J., Environ. Sci. Tech., 5, 422 (1971).

Godt, H.C., Jr., Quinn, J.F., J. Am. Chem. Soc. 78, 1461 (1956).

Hecht, T.A., Seinfeld, J.H., Environ. Sci. Tech., 6, 47 (1972).

Hill, A.C., J. Air Pollution Control Assn., 21, 341 (1971).

Holmes, J.R., O'Brien, R.J., Crabtree, J.H., Hecht, T.A., Seinfeld, J.H., "Measurement of Ultraviolet Radiation Intensity in Photochemical Smog Studies," Submitted to Environ. Sci. Tech. (1972).

Hunter, J.S., "Some Applications of Statistics to Experimentation," Chem. Eng. Prog. Symp. Series, No. 31, Vol. 56, p. 10 (1956).

Johnston, H.S., Pitts, J.N., Jr., Lewis, J., Zafonte, L., Mottershead, T., "Atmospheric Chemistry and Physics," Project Clean Air, Vol. 4, Univ. of Calif., Sept. 1, (1970).

Lee, R.E., Jr., Patterson, R.K., Crider, W.L., Wagman, J., Atmospheric Environment, 5, 225 (1971).

Leighton, P.A., Photochemistry of Air Pollution, Academic Press, New York, N.Y., (1961).

REFERENCES (Continued)

Morris, E.D., Jr., Niki, H., J. Phys. Chem., 75, 3640 (1971).

Schuck, E.A., Stephens, E.R., Schrock, P.R., J. Air Pollution Control Assn., 16, 695 (1966).

Seinfeld, J.H., Hecht, T.A., Roth, P.M., "A Kinetic Mechanism for Atmospheric Photochemical Reactions," App. B of "Development of a Simulation Model for Estimating Ground Level Concentrations of Photochemical Pollutants", 71-SAI-9, Systems Applications Inc., Beverly Hills, Calif. (May 1971).

Westberg, K., Private Communication (1972).

Wilson, W.E., Jr., Private Communication (1972).